Gain/Dipole
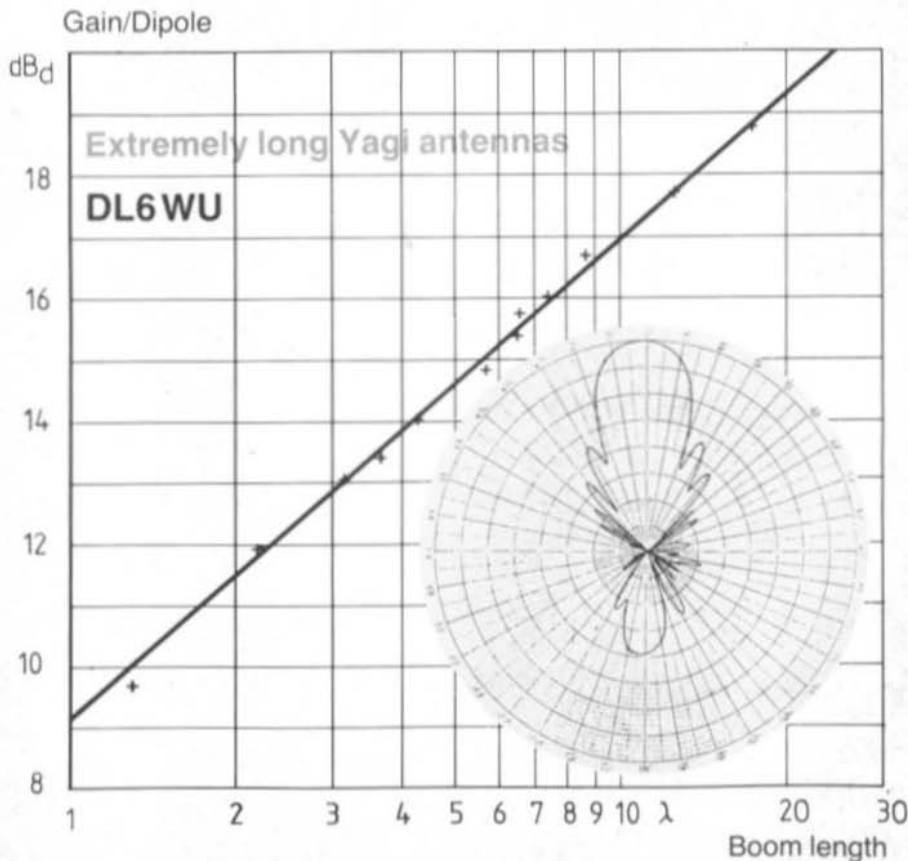
dB_d

Extremely long Yagi antennas

DL6WU

Boom length

# VHF communications

A Publication for the Radio Amateur
Especially Covering VHF, UHF, and Microwaves

Volume No.14 · Autumn · Edition 3/1982

# Contents

# In the Focus

Being a telecommunications engineer, I can see the large gap which exists between professional and radio-amateur technology. In this context I mean the techniques we as radio amateurs are able to apply in home-brew projects, not the technique we can buy. I regret this situation, because it is not our role in history. In some cases however, we have the opportunity to catch up with first-line developments. For such a lucky situation several positive going pulses must coincide: One of our fellows can combine profession and hobby, he has access to some new development, he finds superiors who support his activities, and he finally finds the time to publish his material. This has been the case with Guenter Hoch, DL 6 WU, of the Deutsche Bundespost and we now can again read one of his excellent articles on antennas.

Other examples of »professionals« are Bernd Neubig, DK 1 AG, or Friedrich Krug, DJ 3 RV, who lead us the way to first-grade technology. Next year we will have the luck to read about »Spread-Spectrum Techniques« in a further attempt to learn more about modern telecommunication techniques (remember CCW). VHF COMMUNICATIONS will also focus on picture reception and manipulation techniques, so that radio amateurs can play their role.

With kind 73s

your's

DL 3 WR

*Günter Hoch, DL 6 WU*

# Extremely Long Yagi Antennas

In earlier publications (1, 2) the author has discussed Long Yagi-Uda antennas. The longest arrays then tested were less than 10 wavelengths long. The question of what happens at extreme lengths remained unanswered.

The following article is to give details and data on Yagi beam antennas up to a length of nearly 20 wavelengths !

turation of gain at greater lengths. Later experiments by Viezbicke of NBS (7) confirmed this tendency but showed the saturation to occur only with uniform (equi-spaced equal-element length) arrays.

Element tapering seemed to be the answer, but to what extent would this be valid ? Could element lengths dwindle down to nothing and still provide gain ?

## 1. FUNDAMENTALS OF LONG YAGI ANTENNAS

With the increasing popularity of the UHF bands the problem of cheap and inconspicuous (as compared to parabolic dishes) high-gain antennas has gained importance.

G 3 JVL's well-known Loop Yagi (3) has been a great step in this direction but it has had the side-effect of making many amateurs believe »normal« yagis would not work at GHz frequencies or at these lengths.

There has been evidence in scientific literature, partly dating back to the '50 s, that there should be no major difference in performance of disk, ring, or rod type elements and that arrays tens of wavelengths long were feasible (4, 5).

On the other hand the famous Ehrenspeck yagi-array measurements (6) hinted at a sa-

## 1.1. TAPER PROFILES

Experiments were carried out with various length- and spacing-tapered and uniform arrays. Several conclusions resulted:

### 1.1.1. Uniform Profile

The apparent gain saturation of uniform arrays is probably caused by lack of excitation. If, by means of a tapered »funnel« section, a travelling wave has once been established on the director chain, the remaining portion need not be tapered to reach maximum possible gain. However, as length is added, the side-lobes increase in strength. When they exceed a level 13 dB below the main lobe the addition of further equal length directors causes the frequency of maximum gain to shift downward, necessitating a re-design. Bandwidth decreases quickly with increasing array-length.

### 1.1.2. Linear Taper

If a linear taper is used throughout, reducing the length of each succeeding element by a constant amount, sidelobes tend to decrease in strength as elements are added. When sidelobe attenuation exceeds 19 dB, excessive widening of the main lobe occurs and gain falls short of the possible maximum. The frequency of optimum performance shifts upward. Bandwidth is larger than with uniform or quasi-uniform (funnel-type) arrays and remains fairly high even at great array lengths (8).

These effects are more or less pronounced, depending on the taper rate chosen, but in any case the solution is valid for a limited range of array lengths.

### 1.1.3. Logarithmic Taper

In search of a »universal formula« which permits stopping at any desired array length without shifting the optimum frequency , a logarithmic taper was tried.

The transition section needed to get the travelling wave started, had been determined in earlier experiments. This section is tapered in both element lengths and spacings.

Spacing cannot be increased much beyond 0.4 wavelengths without gain sacrifice, so the logarithmic section is length-tapered only with the starting slope given by the transition section. On the equispaced part of the director chain, the length ratio between elements no. n and 2n is always kept constant. This profile doesn't dwindle to nothing (at least not on finite arrays). Optimum frequency remains constant and sidelobes stay around − 17 dB for any chosen array length.

## 1.2.
## BANDWIDTH

It has been written many times that very long Yagi arrays suffer from extremely low bandwidth, especially if wide spacing is used. Tape-

ring, even at the very modest rates used here, increases bandwidth considerably. The longest array tested (18. wavelengths long) had a − 1 dB-bandwidth in excess of 4 %.

Bandwidth isn't only determined by gain response, however. The second, no less important constituent is matching. By using wideband exciters like folded-dipoles, loops, etc., and avoiding narrow-band (high ratio) impedance transformation, a sufficiently great matching bandwidth can be provided.

## 1.3.
## BOOM INFLUENCE

Several authors have warned not to use metal booms of appreciable thickness, especially with elements not insulated from them. This fear has prompted funny solutions like elements on poles, etc. Both insulated and mounted-through versions were tested by the author. When properly length-corrected **no** difference in performance could be detected. Of course non-insulated elements must be centered and be in good, lasting contact with the boom ! The shortening effect itself was found to be somewhat less than anticipated, not surpassing 2/3 of a reasonably thick boom's diameter.

## 1.4.
## SKIN EFFECT

With increasing frequency skin effect losses are known to rise. They are partly compensated for by decreasing resonant length of elements.

No significant difference could be measured between aluminium, copper, and silver-coated elements. At GHz frequencies high specific resistance materials like brass should be avoided or used for thick elements only. (Brass tubing is not recommended for outdoor application because it tends to crack up).

Gain over dipole
dB_d
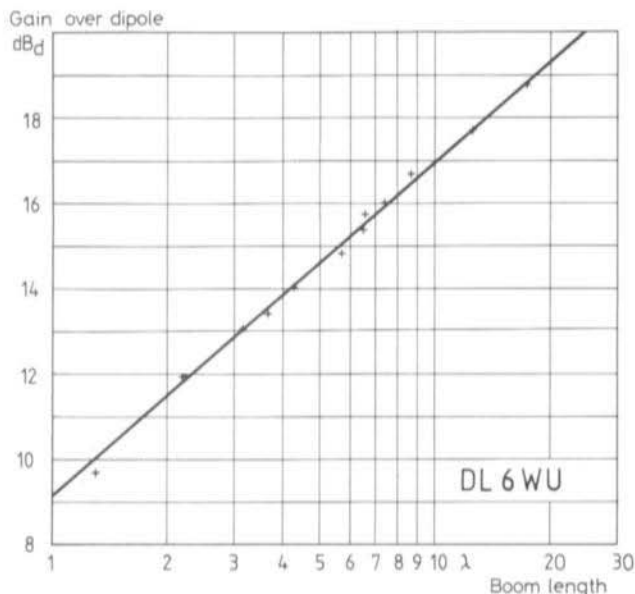
Fig. 1:
Gain of Yagi antennas
measured by DL 6 WU
at 432 MHz and 1296 MHz
(October 1981)

DL 6 WU

Boom length

## 1.5. GAIN

While it was clear now that gain keeps on rising at great arry length, the absolute values still seemed debatable.

Although space requirements for antenna ranges are greatly alleviated at UHF, other problems associated with stability, cable and connector losses, reflexions etc. become more prominent. At 23 cm window-panes can reflect like sheet-metal ! The author's experience with gain measurements at »lower« frequencies was helpful in preliminary back-yard work but serious measurements had to be postponed until recently when a professional antenna measuring range, owned by the German Federal Post Office, became available.

Using an EIA standard gain aerial (7.7 dBd) as a reference many pattern and gain measurements were made on 432 and 1296 MHz. The 70 cm results were consistent with earlier anechoic-chamber values and the 23 cm gain figures line up perfectly with them. Accuracy is believed to be within 0.5 dB.

Figure 1 shows the slightly sub-proportionate increase of gain with array length, the rate of 2.35 dB per octave is in good agreement with earlier measurements on shorter arrays. There is no sign of saturation so it can be expected that further extrapolation be permissible.

## 2.
## PRACTICAL DESIGN

Of course, antenna constructors prefer »hard data« in the form of tables containing all dimensions but it seems impossible to provide such data for all thinkable applications.

So only two typical examples will be described in some detail while experimenters are referred to the graphs given in Figure 2. After all, these super-long yagis aren't as critical as many people used to think !
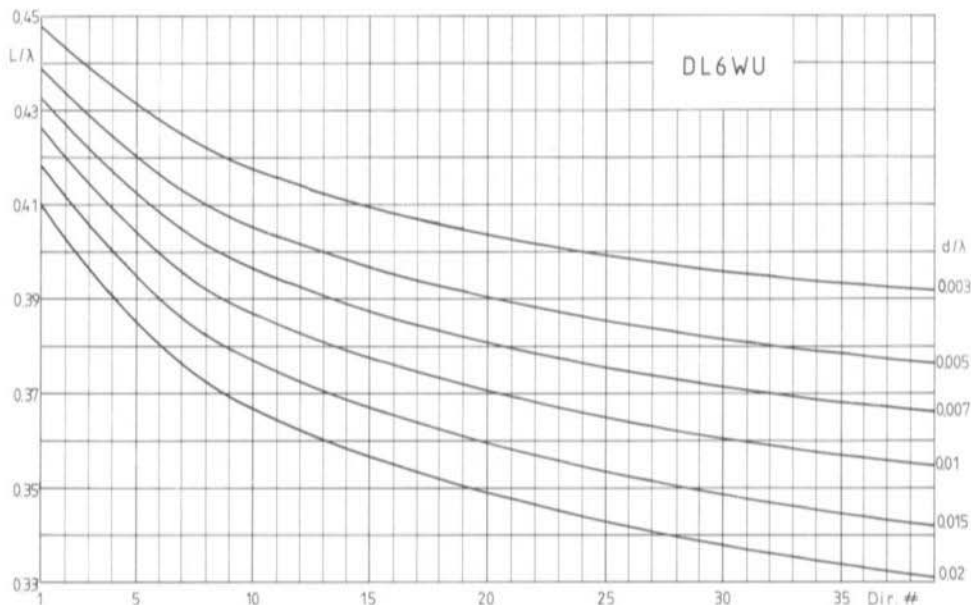
Fig. 2: Optimum director lengths (standardized). Parameter: standardized director diameter

A few checks to be given later should assure even the less-experienced builder without intricate test equipment that his array is working correctly.

## 2.1.
## A 23 ELEMENT YAGI FOR 432 MHz

A long-boom model was constructed using TV aerial material and parts **(Table 1)**.

All elements are 10 mm ⌀ aluminium tubing mounted on a 20 x 20 mm square boom by means of plastic insulators. Separation is about 4 mm which nearly eliminates the boom influence. Folded dipoles are very uncritical with respect to element thickness, limb and end separation, so any dipole box at hand can be used. Feed point impedance is near 200 Ω so a 4:1 coax balun provides a good match to 50 Ω coaxial cable.

| Element | Length | Distances |
|---|---|---|
| Reflector | 330 | 130 |
| Driven El. | 325 | — |
| Director  1 | 295 | 55 |
| Director  2 | 290 | 125 |
| Director  3 | 285 | 150 |
| Director  4 | 280 | 195 |
| Director  5 | 275 | 195 |
| Director  6 | 275 | 210 |
| Director  7 | 270 | 220 |
| Director  8 | 270 | 230 |
| Director  9 | 265 | 240 |
| Director 10 | 265 | 250 |
| Director 11 | 265 | 260 |
| Director 12 | 260 | 260 |
| Director 13 | 260 | 270 |
| Director 14 | 260 | 280 |
| Director 15 | 260 | 280 |
| Director 16 | 258 | 280 |
| Director 17 | 258 | 280 |
| Director 18 | 258 | 280 |
| Director 19 | 255 | 280 |
| Director 20 | 255 | 280 |
| Director 21 | 250 | 280 |

Table 1:
Dimensions of a 23 element Yagi antenna for 432 MHz using insulated 10 mm elements

## 2.1.1. Performance

Gain of the 23 element long-boomer was measured to be 16.0 dB over a dipole. Half-power beamwidth in both planes varies between 22°

and 24° across the 70 cm band (430-440 MHz). **Fig. 3a and 3b** show the original diagrams measured at 433 and 439 MHz, resp.
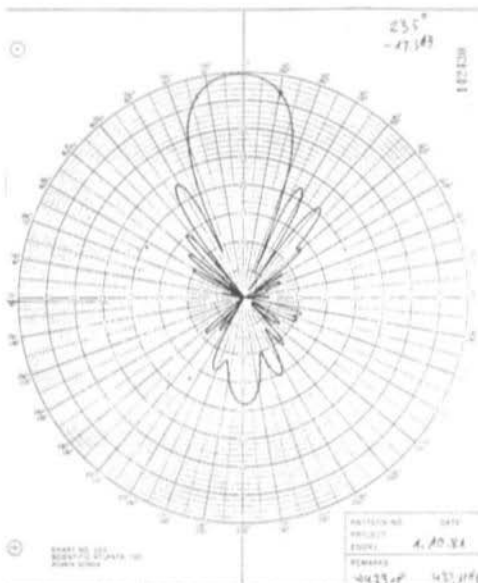


Fig. 3a:
E-plane diagram of the 70 cm antenna
with 23 elements at 433 MHz
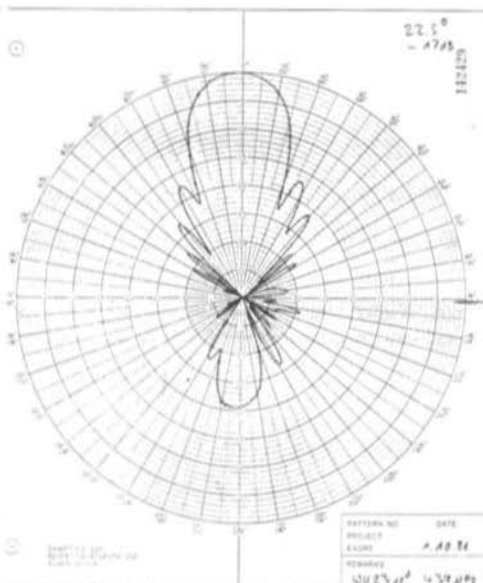
Fig. 3b:
As Fig. 3a but measured at 439 MHz

## 2.2.
## A 49 ELEMENT YAGI FOR 1296 MHz

Material chosen for the long-boom 23 cm array was 4 mm ∅ hard aluminium for the elements (AlMg5 welding electrodes) and 1/2" (12.7 mm) alu tubing for the boom. The latter is readily available at hardware stores.

A supporting structure is necessary to keep the boom from sagging and to keep the bulky mast clamp at least a wavelength away from the elements.

### 2.2.1. Feed Arrangements

Several feeds were tried with more or less sa-

tisfactory results. While a stepped-diameter folded dipole soldered directly to a hardline balun and a folded dipole with integral three-wire symmetry transformer proved best, the rather simple solution shown in **Figure 4** was nearly as effective (about 1/4 dB extra loss).

### 2.2.2. Element Mount

Elements must be centered to better than 1 mm and have good contact to the boom. 3 mm ∅ holes were drilled and then widened to 3.9 mm from both sides (to avoid a loose fit in the »upper« hole). Elements were then driven in with a hammer.
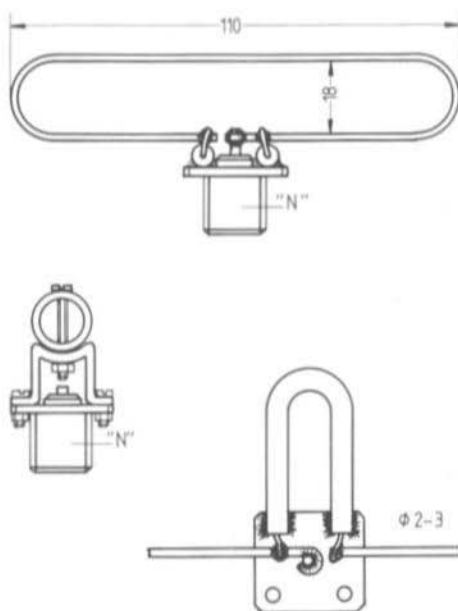
Fig. 4:
23 cm balun arrangement from semi-rigid cable.
Balun length (outer conductor): 80 mm

| Element | Length | Distances |
|---|---|---|
| Reflector | 118 | 50 |
| Driven El. | 110 | – |
| Director 1 | 104 | 18 |
| Director 2 | 102.5 | 42 |
| Director 3 | 101 | 50 |
| Director 4 | 99,5 | 58 |
| Director 5 | 98 | 65 |
| Director 6 | 97 | 70 |
| Director 7 | 96 | 73 |
| Director 8 | 95 | 76 |
| Director 9 | 94 | 80 |
| Director 10 | 94 | 83 |
| Director 11 | 93 | 86 |
| Director 12 | 93 | 90 |
| Director 13-15 | 92 | 92 |
| Director 16-18 | 91 | 92 |
| D+irector 19-21 | 90 | 92 |
| Director 22-24 | 89 | 92 |
| Director 25-28 | 88 | 92 |
| Director 29-32 | 87 | 92 |
| Director 33-37 | 86 | 92 |
| Director 38-43 | 85 | 92 |
| Director 44-47 | 84 | 92 |

Table 2:
Dimensions of a 49 element Yagi antenna for
1296 MHz using 4 mm elements through a 1/2"
(12 mm) boom

## 2.2.3. Dimensions

**Table 2** gives element lengths and spacings. Although spacings are not overly critical they should be checked »from both ends« especially if several identical arrays are to be built.

## 2.2.4. Performance

With the feed shown, a gain of 18.8 dB over a dipole was measured, so probably 19 $dB_d$ are within reach. E- and H-plane beamwidths were measured to be 15°. **Fig. 5** shows the original diagram.

## 2.3.
## IMPROVED REFLECTORS

Very long Yagis inherently have a high front-to-back ratio. It should be remembered, however, that pickup from behind can be considerable, in absolute terms. 21 dB F/B in a 16 dBd gain array means that the rear lobe is just 5 dB below dipole level. If this is considered insufficient — for instance in EME work — several improvements over the single reflector version are possible.

### 2.3.1. Dual In-line Reflector

This arrangement, made popular by Dick Knadle, K 2 RIW, can be applied to nearly any Yagi aerial: A second, slightly longer, reflector is added about 0.5 wavelengths behind the first. This improves the F/B ratio some-what and adds up to 0.2 dB to forward gain. Match remains unaltered.

Fig. 5:
E-plane diagram of the 23 cm antenna with
49 elements and a gain of 18.8 dB$_d$

## 2.3.2. Multiple Reflectors

Instead of a single reflector element an array of reflectors in a plane perpendicular to the boom can be used. A double reflector should be spaced 0.3 λ vertically and approx. 0.15 to 0.2 λ behind the radiator. Length should be slightly greater than for the single reflector. 4 reflectors spaced about 0.2 λ and approx. 0.6 λ long will improve F/B ratio further.

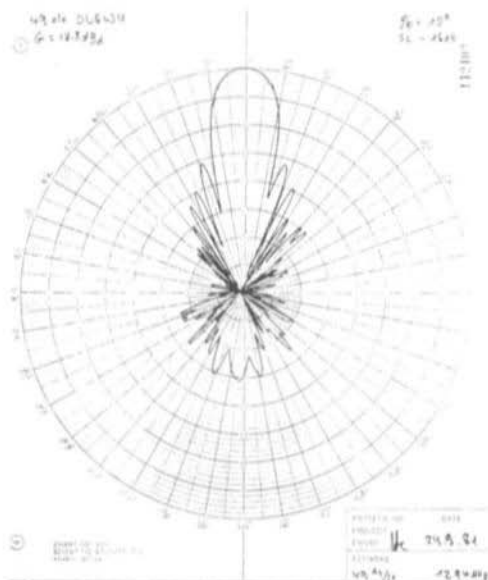The additional gain will normally not exceed 0.2 dB with any of the arrangements mentioned. No serious matching problems should arise, usually the multiple reflectors tend to raise the impedance somewhat and to broaden the response toward lower frequencies.

## 2.3.3. Reflector Planes

A metal sheet or grid 0.6 λ wide and high can replace a quadruple reflector with no change in performance.

# 3.
# CHECKING THE PERFORMANCE

The most significant feature of any antenna is its radiation pattern. So even a rough check can tell a lot about performance. Yagi patterns possess characteristic features which are helpful in performance tests.

At array lengths beyond about 7 wavelengths E and H patterns become almost identical, at least around the boresight axis, so it is sufficient to test one plane — usually E.

If the array works properly there are pronounced nulls between main lobe and first sidelobes. The angle between these first nulls is very close to twice the aperture angle or half-power beamwidth (slightly larger in the E plane). With the profiles given here the first sidelobes should be suppressed by about 16-17 dB.

At frequencies below optimum the main lobe widens with only minor changes in the pattern's appearance, except that the first nulls become deeper. Gain decreases slowly.

When the optimum frequency is exceeded, the first nulls quickly fill in and the first sidelobes begin to merge with the main lobe, increasing in amplitude. The main lobe becomes narrower at the tip despite quickly decreasing gain. Patterns 3a and b show first signs of the effects mentioned — optimum operating frequency is near 436 MHz.

If the radiation patterns look like the ones shown and there is no serious mismatch (1:1.3 at feedpoint or better), one can be sure tha performance is correct.

# 4.
# STOCKING

After it has been assured that single arrays are working correctly they can be grouped in the usual manner.

## 4.1.
## OPTIMUM SPACING

For beamwidths $\Phi$ below about 30° the optimum stacking distance $D_{opt}$ is with sufficient accuracy:

$$D_{opt} = \frac{57.3\,\lambda}{\Phi}$$

For the 23 ele array with $\Phi \approx 24°$

$D_{opt}$ is 2.39 $\lambda$ or 1.66 m at a wavelength of 70 cm. With the 49 ele array ($\Phi \approx 15°$)

$D_{opt} \approx 3.82\,\lambda$ or 0.9 m at wavelength of 23 cm.

## 4.2.
## MAST CLEARANCE

No conducting structures should run between elements if they are thicker than about $\lambda/10$. Metal structures parallel to the elements should be kept at least half the stacking distance away.

## 5.
## OWN DESIGNS

Using the graphs in Figure 2, long Yagis can be designed for any frequency and for a wide range of length and element dimensions.

## 5.1.
## SCALING

Scaling is done by first calculating the element diameter/wavelength ratio at design center frequency and then reading off the director lengths from Fig. 2. If elements run through a metal boom uninsulated, 66 % of boom diameter must be added.

Folded dipole and reflector elements can be scaled from the dimensions given here as their lengths are almost independent of element diameter.

Spacings should also be scaled from the dimensions given here, inversely proportional to the frequencies.

## 5.2.
## PERFORMANCE

Gain to be expected can be estimated from Figure 1, which relates gain to array length. Radiation patterns given for the two model arrays indicate the beam pattern to be expected. The front-to-back ratio fluctuates with array length with minima about 2 dB below dipole level. It can always be improved by the measures mentioned in chapter 2.3. Bandwidth shows only a very slight tendency to decrease with growing length and should remain more than 3% even for the longest manageable arrays.

## 5.3.
## EXTENSION

If it is desired to continue beyond the dimensions given, extrapolation should follow the logarithmic law, keeping constant the length ratio between elements no. n and 2n. The checks named in chapter 3 should suffice to assure optimum performance.

## ACKNOWLEDGEMENT

# 6.
## REFERENCES

(1) Hoch, G.: Yagi Antennas
VHF COMMUNICATIONS 9, 3/1977,
Pages 157-166

(2) Hoch, G.: More Gain with Yagi Antennas
VHF COMMUNICATIONS 9, 4/1977,
Pages 204-211

(3) Evans, D.S. and Jessop, G.R.:
Long Quad Yagi for 1296 MHz
RSGB VHF-UHF Manual, 3rd Edition,
Pages 8.48-8.49

(4) Simon, J.C., and Biggi, V.:
Un Nouveau Type d'Aérien ...
L'Onde Electrique 34, 1954,
Pages 883-896

(5) Appel-Hansen, J.: The Loop Antenna
with Director Arrays of Loops and Rods
IEEE Trans.Ant.Prop., Juli 1972,
Pages 516-517

(6) Ehrenspeck, H.W., and Poehler, H.:
A New Method for Obtaining Maximum
Gain from Yagi Antennas
IRE Trans.Ant.Prop., Oct. 1959,
Pages 379-386

(7) Viezbicke, P.P.: Yagi Antenna Design
NBS Technical note no.688, Dec.1976
(summarized in HAM Radio, Aug.1977,
Pages 22-31)

(8) Sengupta, D.L.: On Uniform and
Linearly Tapered Yagi Antennas
IRE Trans.Ant.Prop., Jan. 1960,
Pages 11-17

*The Editors*

# Using the GaAs-FET S 3030 in a 70 cm Preamplifier

The interest shown in the 144 MHz pream-
plifier equipped with the S 3030 has led to
the development of a similar amplifier for
432 MHz. Discussions with DL 9 JU and
DJ 1 SK at the 1982 VHF-UHF Conference
in Munich gave valuable assistance. The
described prototype operated with less
problems than a BF 981 preamplifier for the
144 MHz band !

## 1. CONSIDERATIONS

All prototypes of this preamplifier exhibited
noise figures between 0.7 and 0.8 dB when
measured on an automatic noise system.
Lower noise figures for EME operation can
only be obtained when using microwave GaAs
FETs such as the MGF 1400 (approx. 0.5 dB)
or the MGF 1412. However, these transistors
cost approximately 4 to 8 times more than the
S 3030.

Noise figures below 1 dB are also possible
when using bipolar transistors: For instance
0.6 dB can be obtained when using the NE
64535. Whe using the new BFQ 69 manufac-
tured by Siemens, it will be possible to obtain a
noise figure of 0.8 dB at 432 MHz when using a

wideband circuit from 80 to 470 MHz (loss-less
feedback circuit as described in [2]). However,
the latter does not have any selectivity; this
can, of course, be realized using a previous fil-
ter, however, an insertion loss of only 0.5 dB
can deteriorate the noise figure by up to 6 dB !
Such circuits are often very difficult to align to
minimum noise even when a large amount of
measuring equipment is available.

These problems are solved by using a dual-
gate FET such as the BF 981 or the S 3030.
These transistors have such a high impedance
at the gate that the input noise matching can
be easily realized with the aid of a parallel
resonant circuit with tap, which also provides
selectivity.

## 2. CONSTRUCTION

The circuit given in **Figure 1** and the construc-
tional drawing given in **Figure 2** show all im-
portant details required for construction. The
30 mm high case can be constructed from PC-
board material or brass plate. Do not forget to
provide the hole for the transistor in the inter-
mediate panel.
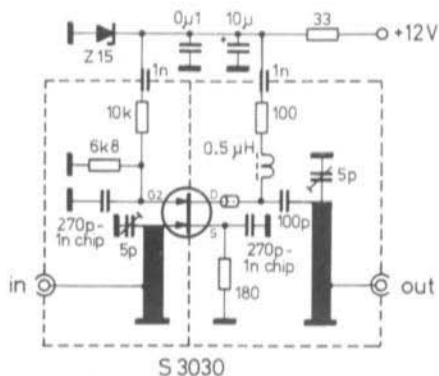
Fig. 1:
This 70 cm preamplifier is equipped with a S 3030 GaAs-double gate MES-FET. The drain current is 11 mA and the noise figure is approximately 0.7 dB.

The highest possible Q should be provided at least at the input side, and for this reason, the input conductor (6 mm brass tube) should be silver-plated and glass tubular trimmer of 5 pF (Johanson or Tekelec Airtronic) should be

used. If not available, it will be possible to use a ceramic tubular trimmer (Philips). On the other hand, a ceramic trimmer is sufficient on the output side. The length of the inner conductor (approx. 70 mm) depends on the trimmers used.

The connections of source and gate 2 are soldered onto ceramic chip capacitors in a similar manner to that described for the 144 MHz version in (1). The capacitance value is uncritical and may be between approximately 270 pF and 1 nF. The ferrite bead on the drain connection is provided to avoid high frequency oscillation in conjunction with the choke-resistance combination of the drain voltage.

The DC-voltages for drain and gate 2 are fed into the chambers with the aid of feed-through capacitors whose capacitance value is less important than their UHF quality. The transistor is protected against overvoltages with the aid of the zener diode. It is not operative at the normal voltage of 12 V. The transistor should be handled in the same way as a C-MOS component.
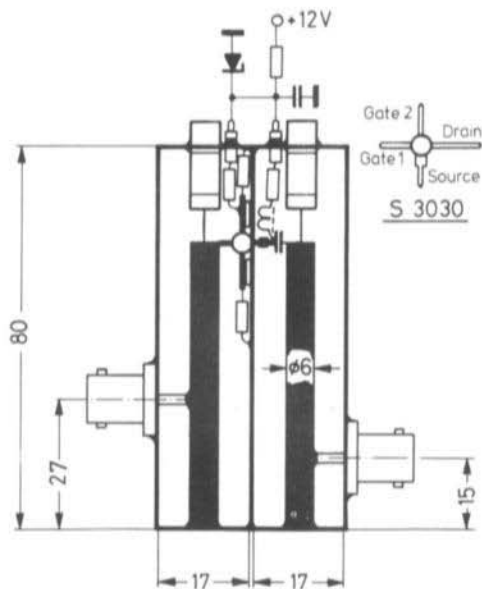


Fig. 2:
The chamber-type construction is used to provide the highest Q and optimum screening. The input circuit should be provided with a silver-plated inner conductor and a glass tubular trimmer.

# 3.
# ALIGNMENT

Firstly carry out a DC-check by measuring the voltage drop across the source resistance. It should amount to approximately 2.0 V. If the measured value differs greatly from this, vary the value of one of the two gate-2 resistances.

After closing the case, both trimmers are now aligned for maximum gain. Finally, the input trimmer is inserted somewhat (towards higher capacitance) until the sensitivity (signal-to-noise ratio) is optimized. Of course, this can be achieved most easily when using an automatic noise figure system, however, it can be optimized at first with the aid of a very weak FM-signal that is monitored in an FM-receiver with the squelch switched off. If the signal level is in the correct range, the slightest variations of the UHF signal-to-noise ratio will be clearly heard as variations of the AF-signal-to-noise ratio.

## 3.1.
## MEASURED VALUES

Noise figure NF  $=$  0.7 dB

Gain A  $=$  22 dB
Drain current $I_D$  $=$  11 mA
Input intercept point $IP_i$  $=$  0 dBm

## 4.
## REFERENCES

(1)  Editors:
     Using the Dual-Gate GaAs-FET S 3030
     in a Low-Noise Preamplifier for 144 MHz
     VHF COMMUNICATIONS 14
     Edition 2/1982, pages 77-80

(2)  M. Martin, DJ 7 VY:
     A New Type of Preamplifier for 145 MHz
     and 435 MHz Receivers
     VHF COMMUNICATIONS 10
     Edition 1/1978, pages 30-36

# New Interdigital Bandpass Filters

**4-stage, sealed bandpass filters for
1152 MHz, 1255 MHz, 1288 MHz or 1297 MHz
centre frequencies.**

| | |
|---|---|
| 3 dB bandwidth: | 12 MHz |
| Passband insertion loss: | 1.5 dB |
| Attenuation at ± 24 MHz: | 40 dB |
| Attenuation at ± 33 MHz: | 60 dB |
| Return loss: | 20 dB |
| Dimensions (mm): | 140 x 70 x 26 |

Ideal for installation between first and second pre-amplifier or in front of the mixer for suppression of image noise, and interference from UHF-TV transmitters and out-of-band Radar Stations. Also very advisable at the output of a frequency multiplier chain, or behind a transmit mixer.
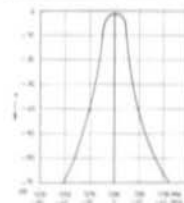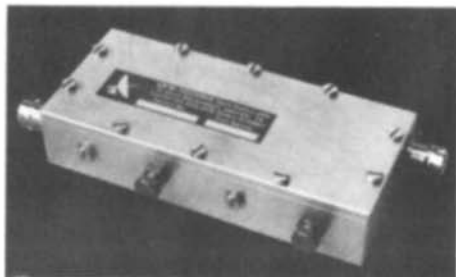




**Price:   DM   168.—**

Please list required centre frequency on ordering.

Klaus Dieter Bröker, DK 1 UV

# A Power Amplifier for 3456 MHz Equipped with a YD 1060 Tube

A power amplifier stage for the 9 cm band was developed after a considerable amount of experiments on resonator types and tube contacts. This power amplifier was able to match the specifications of the tubes in conjunction with satisfactory current and voltage values.

Figure 1 shows a tube-stage power amplifier equipped with two tubes YD 1060, as seen from the driver side. Figure 2 shows the same amplifier from the antenna output complete with power supply, fan, and two meters for the anode currents.
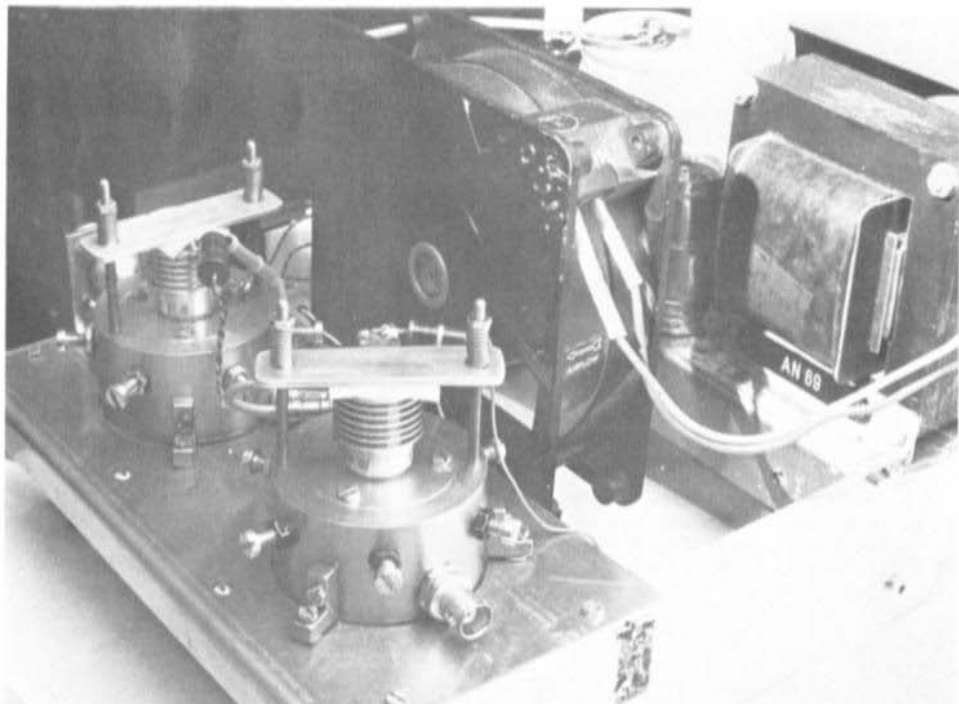


Fig. 1: A two-stage power amplifier for 3456 MHz (9 cm band)
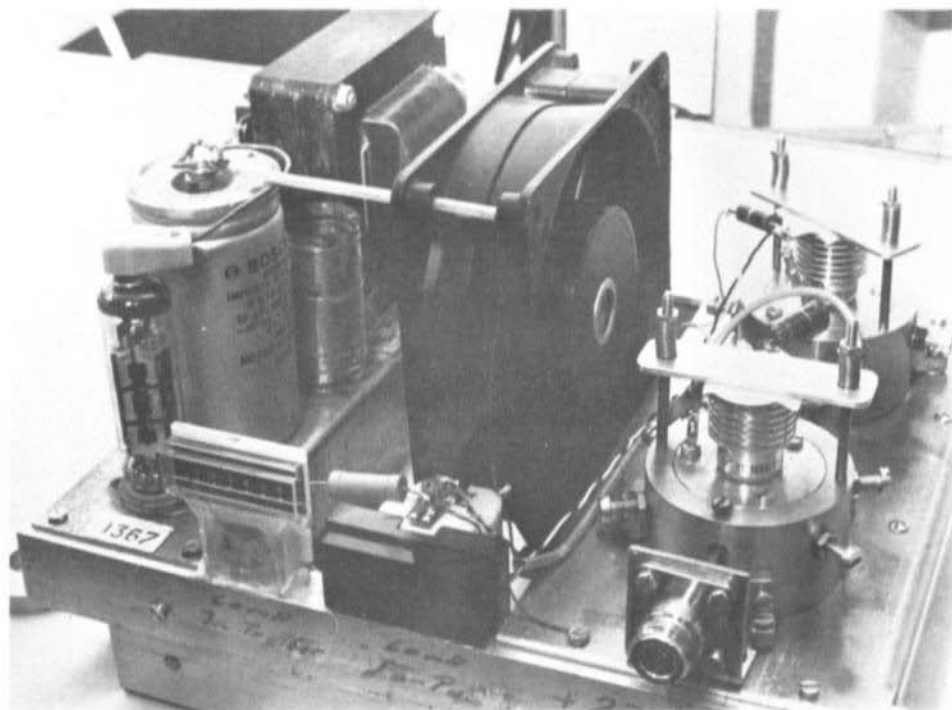
Fig. 2: The YD 1060 tubes are pressed on to the grid connection using a pressure plate and springs

## CONTACTS

All attempts to use conventional contact strip material on the 9 cm band were without success. It is assumed that the conductor inductance due to the very long springs is too high at this wavelength, which means that the tube can no longer be tuned to resonance. For this reason, the holes for the grid and anode ring are fitted exactly to the tube so that the low residual gap at the grid connection can be made with the aid of conductive silver, and be filled with the aid of the thin PTFE-foil of the bypass capacitor at the anode connection. The actual grid connection is, however, made by surface pressure of the grid ring onto the lathed piece. The bypass capacitor at the anode which is connected between anode ring and cover of the resonator provides a capacitance of approximately 70 pF when using a 0.01 mm PTFE-foil. This represents a capacitive impedance of only approximately 0.66 $\Omega$.

## TUNING THE ANODE RESONATOR

Figure 3 gives an impression of the construction of the power amplifier. The tuning of the anode resonator is made inductively with the aid of the five tuning screws mounted around the circumference. Without the screws, the resonance will be at a lower frequency (approx. 3380 MHz), and is dependent on the anode/grid capacitance. On inserting the five screws

143

DK 1 UV



Insulating material

Spring

M 3 threaded bar

Metal plate
approx. 15 mm wide, 3 mm thick

YD 1060

PTFE 0.01 mm foil
Bypass cap. ≈ 70 pF

Anode resonator

5 pcs. M 4 tuning screws

Insert tube using
conductive silver

Cathode resonator

Tuning
(position see
lower view)

Link 3 mm wide

Insulating washer

PTFE 0.1 mm
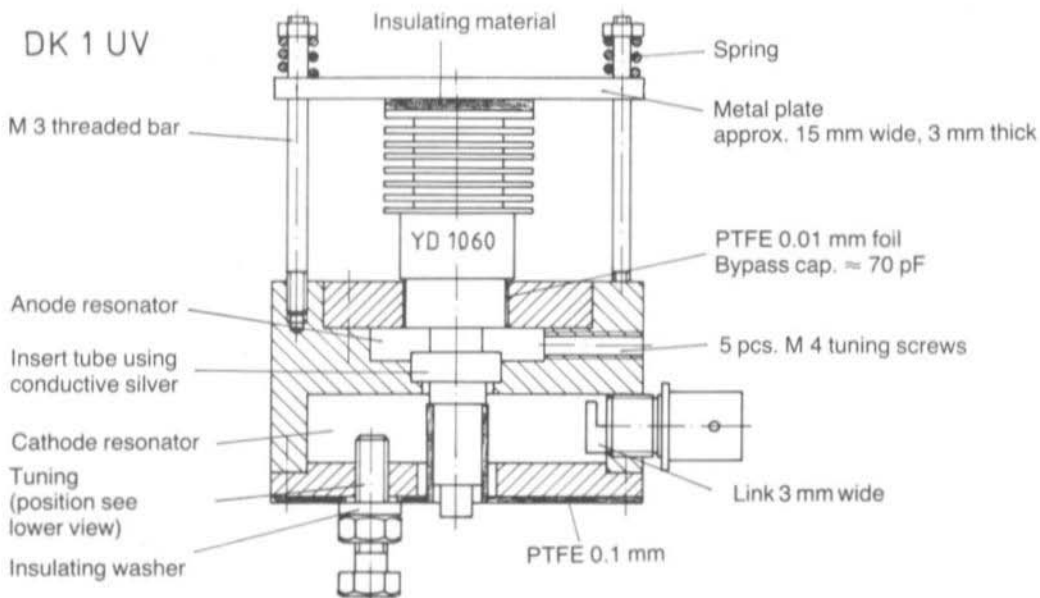
Fig. 3: A 3456 MHz power amplifier with 10 to 14 dB gain (according to output power)

and inserting the coupling link, the resonant frequency will be shifted upwards to a maximum of 3500 MHz.

By alternately correcting the five alignment screws, it is possible to obtain a good symmetrical field in the anode resonator, which is observed as a favorable relationship of output power to DC-power.

## CONSTRUCTION OF THE PARTS

The individual parts shown in **Figures 4-8** are made from brass. The PTFE-foils at the cathode contact plate, and anode ring, as well as the screws, plate, springs, and coupling link are not shown; however, Figures 1 and 3 provide sufficient details.

The output coupling is shown in **Figure 9**. The link comprises an area of approximately 3 mm

x 1.5 mm and is soldered to the end of a piece of semirigid cable. This semirigid cable is placed through the sixth radial hole in the main body, whose diameter should be only just more than that of the cable used. The length of the cable is not important; the other end of the cable is soldered to an N-connector (a flange connector type UG-58 A/U was used in the prototype). The ground connection should be made using a cone (type UG-177/U).

**Figure 10** shows the completed resonator from below and shows the position of the input coupling connector (BNC) and the cathode tuning screw. The cathode resonator is capacitively tuned; the contact between the tuning screw and the cover of the cathode cavity must be very good if a stable operation is to be achieved. For this reason, it is recommended that a fine thread M 6 x 0.5 is used. The tuning behaviour is very sharp.

The lathed pieces and their assembly are finally shown in **Figure 11**.
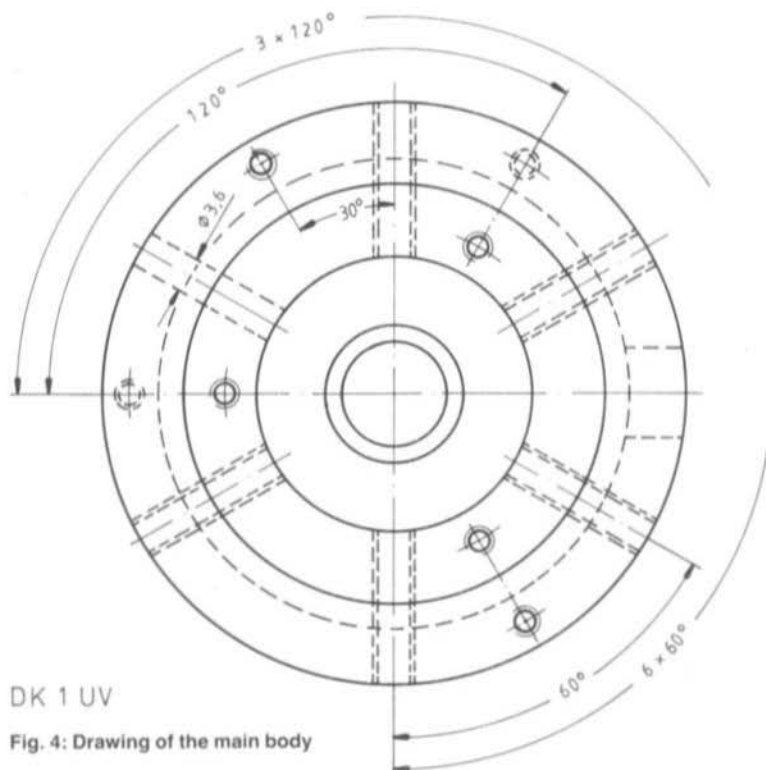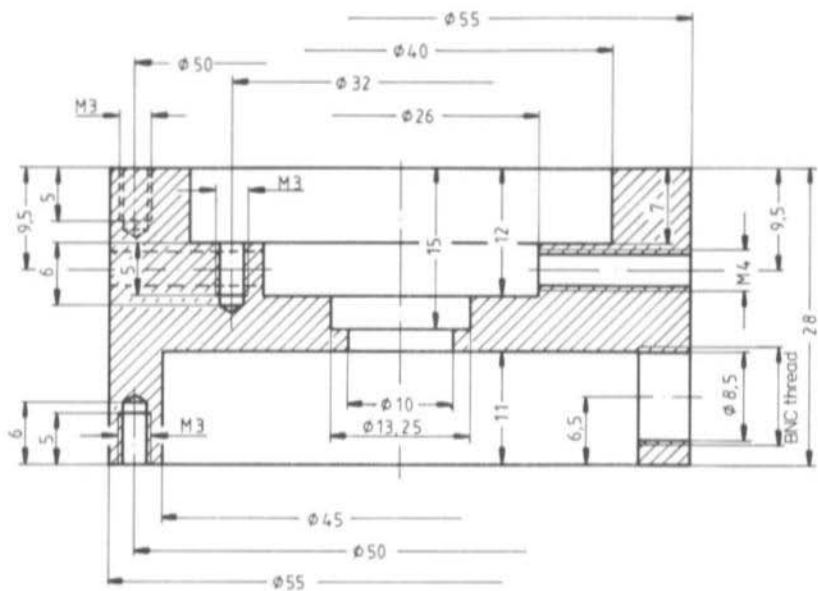
DK 1 UV

Fig. 4: Drawing of the main body
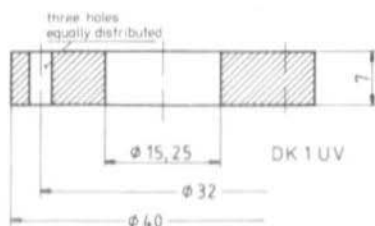
Fig. 5: Cover of the anode cavity
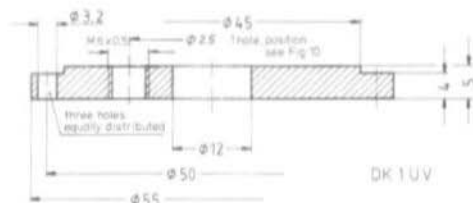


Fig. 6: Cover of the cathode cavity
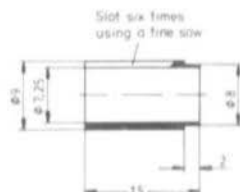


Fig. 7: Cathode contact collar



Fig. 8: Cathode contact plate



Output coupling link
Inner conductor

3.5 mm
Semi-rigid cable

Coaxial cone     N conn.
UG-177/U         UG-58A/U
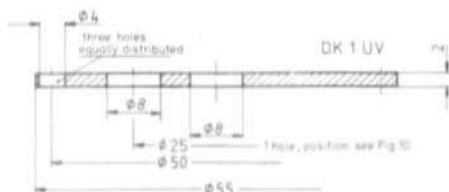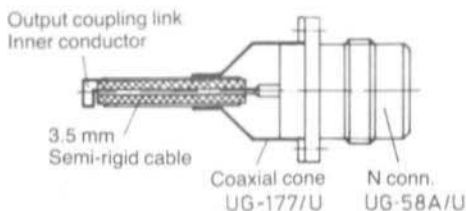
Fig. 9: Output coupling
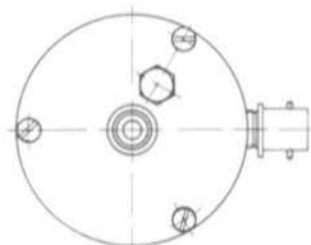


Fig. 10:
View from below; pay attention
to the position of the tuning !

## ALIGNMENT

The heater voltage should not exceed 6 V (see data sheet). The anode current should not exceed 60 mA, since otherwise the inside of the tube will become so hot that it will considerably vary the anode/grid capacitance, which means that it will be necessary to continuously tune the anode resonator. An output power of 6 W can be achieved within these limits, and the described power amplifier operates very stably without retuning. At an output power of 10 W, ($I_a$ = 100 mA) the power amplifier stage was thermally instable and could not be used effectively.

The negative grid bias voltage is made in a conventional manner by inserting a variable constant-voltage two-pole similar to that shown in **Figure 12**.

A microwave power meter with an input impedance of 50 $\Omega$ is now connected to the output socket and the anode current aligned to 30 mA with the aid of the trimmer potentiometer (Fig. 12). All five tuning screws on the anode resonator are now temporarily inserted by approximately 1 mm. The drive signal is now switched on, and the cathode resonator tuned. The tuning screw finally protrudes approximately 1 mm into the resonator; under resonance conditions, it should be possible to measure a slight output power at the output. Finally, the anode resonator is tuned and trimmed carefully for maximum SHF-output power.
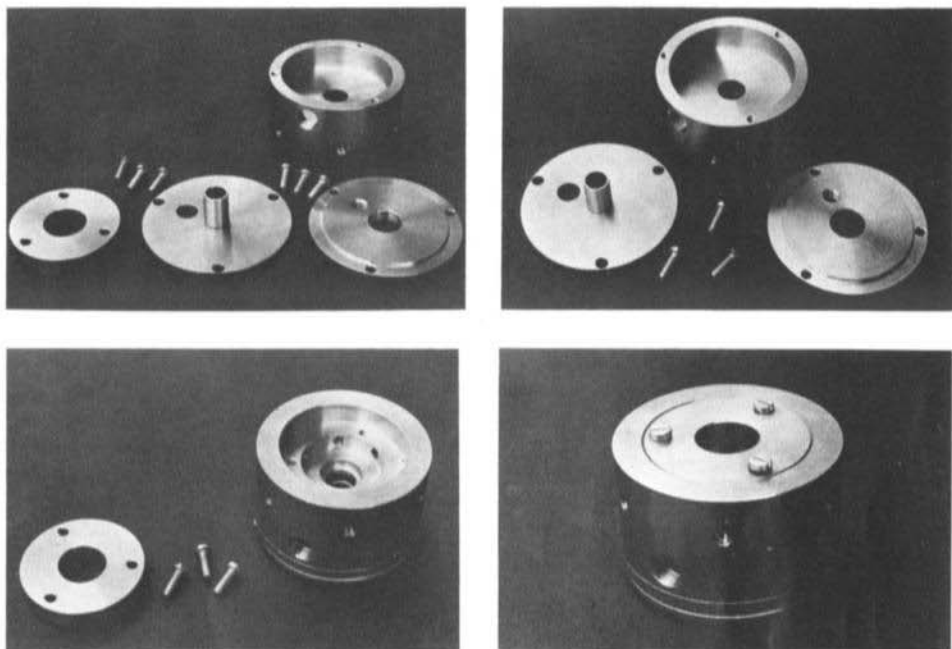
Fig. 11:   Assembly of the lathed pieces

The insertion depth of the coupling link deter-mines the gain of the stage. Under small-signal conditions, a gain of 16 dB can be achie-ved. The specifications are:



Fig. 12

$U_a$ = 400 V                        $I_a$ = 40 mA
$P_{in}$ = 20 mW              $P_{out}$ = 800 mW

A tendency to self-oscillation or instability will be noticed at higher gain levels, and this will be audible as distorted SSB-signals.

At higher output powers, the gain per stage will be reduced to approximately 10 dB due to the close-coupled output coupling. The author's prototypes shown in Figure 1 are connected in series and exhibit an overall gain of 24 dB with an output power of 6 W. The driver stage is run with $U_a$ = 200 V and $I_a$ = 40 mA, and the output stage with $U_a$ = 400 V and $I_a$ = 25 mA. The cur-rent values are quiescent current, which in-crease to 55 mA under full drive conditions.

147
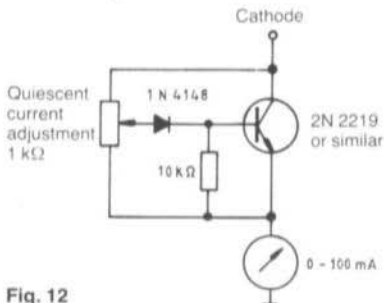
*Jan M. Noeding, LA 8 AK*

# Bias Voltage Circuit for Tubes of the 2 C 39 / 3 CX 100 Families

A common circuit for generating the requir-
ed grid bias voltage for tubes of the 2 C 39
and 3 CX 100 (A) family was described in
(1) and is given again in **Figure 1.** In this cir-
cuit, only the very low base current of the
transistor flows through the diode, which
means that it operates in an unfavourable,
curved range of its characteristic. For this
reason, cathode current fluctuations can
be noticed as bias voltage fluctuations.

The improved circuit shown in **Figure 2** allows
the diode to be connected in the emitter circuit.
The higher current now flowing through the
diode shifts its operating point into the steeper
part of the characteristic so that only low fluc-
tuations of the bias voltage result in the case of
cathode current fluctuations.

In addition to this, a solution was sought to indi-
cate the cathode current of one or two tubes on

a meter without making it necessary for a mA-
meter to be connected in the high-voltage line.
In the case of the circuit given in Figure 1, the
meter was connected in the collector circuit.
For construction, however, it seemed simpler
to separate the meter from the actual amplifier
circuit and the bias voltage. The improved cir-
cuit is now shown in Figure 2. In this circuit the
reference voltage remains virtually constant
during operation of the tube(s), and the meter
will have only a very low effect.

The bias voltage generated in the circuit
shown in Fig. 2, can be calculated as follows:

$$U_c = \frac{R\,1 + R\,3}{R\,3} \times I_c$$

$$= (R\,1 + 1\,k\Omega) \times 1.3\,mA$$

With R 1 in $k\Omega$, the resulting cathode voltage
$U_c$ will be in Volt. Resistor R 2 should be se-
lected to suit the meter used.
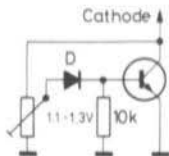
Fig. 1: Conventional bias circuit
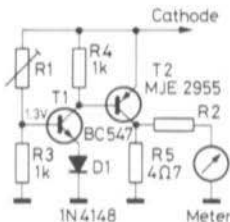
Fig. 2: The bias voltage is independent
of the cathode current

Finally, it should be noticed that it is only necessary for the base of transistor T 1 to be grounded in order to virtually suppress the cathode current flowing via the tube(s). The residual current is then $U_C/R$ 1, and the current flowing via R 3 and R 4 will amount to a total of approximately 2 mA, when T 2 just does not conduct. The measuring error is thus negligible. This type of »cut-off« can be used, for instance, for keying.

In order to achieve a complete blocking, it is necessary for R 1 to be switched off, which can be made using a switching transistor or relay. In order to avoid noise from the power amplifier, a further resistor should be provided, and have approximately 47 kΩ from cathode to ground.

## REFERENCES

(1)  A Tautrim, DJ 2 PU:
     A Stripline Power Amplifier for 70 cm
     Using a 2 C 39 Tube
     VHF COMMUNICATIONS 4,
     Edition 3/1972, pages 144-157

(2)  K. Weiner, DJ 9 HO:
     A Simple 70 cm Power Amplifier
     Equipped with the 2 C 39
     VHF COMMUNICATIONS 7,
     Edition 2/1975, pages 78-82

*Erwin Schaefer, DL 3 ER*

# A Gunn Oscillator, Detector, and Mixer Module for 24 GHz

The described construction can be used as Gunn oscillator or as detector/mixer in the 24 GHz amateur band. It is a further example of the use of bicycle valves (1) and the previously described choke system for contact-less tuning of waveguide modules. Common semiconductors manufactured by well-known firms such as Siemens, Microwave Associates, etc. are to be used in a waveguide type WR 28 (R 320).

The module partly consists of previously described parts such as a choke mount for the diode feed, and a choke arrangement for the tuning. The construction is very simple, but requires – as mentioned in previous articles – the use of a lathe.

## OPERATING BEHAVIOUR

Due to the high cut-off frequency of the waveguide type WR 28 used, it was possible when using suitable Gunn elements to generate oscillation up into the range of 35 GHz. Of course, it is also possible to use waveguide type WR 42. Electrically speaking, it is only the wavelength in the waveguide that changes, which means that the dimensions can be recalculated from those given in the drawings.

The use of a choke tuning allows a clear maximum to be found both when used as an oscilla-

tor, and as a detector. The conventional Gunn element (lower right) or Schottky diodes (below left) shown in Figure 1 can be used in this module.

## CONSTRUCTION

**Figure 1** shows the complete module, which can be equipped with standard, or home-made flange connectors. For matching, one can use the well-known three-screw tuner (2 mm dia., spacing $\lambda_{wg}/8$ to $\lambda_{wg}/4$) – if this should be required – after which the output side of the module is lengthened by 1 to 2 cm.

In the **parts list**, those parts that can be taken from articles (1) and (2) are marked. Other parts that must be constructed are given in the drawings given in **Figure 2**. Other parts given in the list do not require drawings.

All solder joints are made with soft solder. If a flange is to be installed, it should be firstly soldered to the waveguide using a solder having a high melting temperature. The connection side of the flange can then be finished by milling or lathing. It may be sufficient to finish the surface with the aid of a wet emery cloth which is placed on a glass surface. Attention should be paid to obtain a constant pressure during the finishing process so that the flat surface is not rounded by mistake.
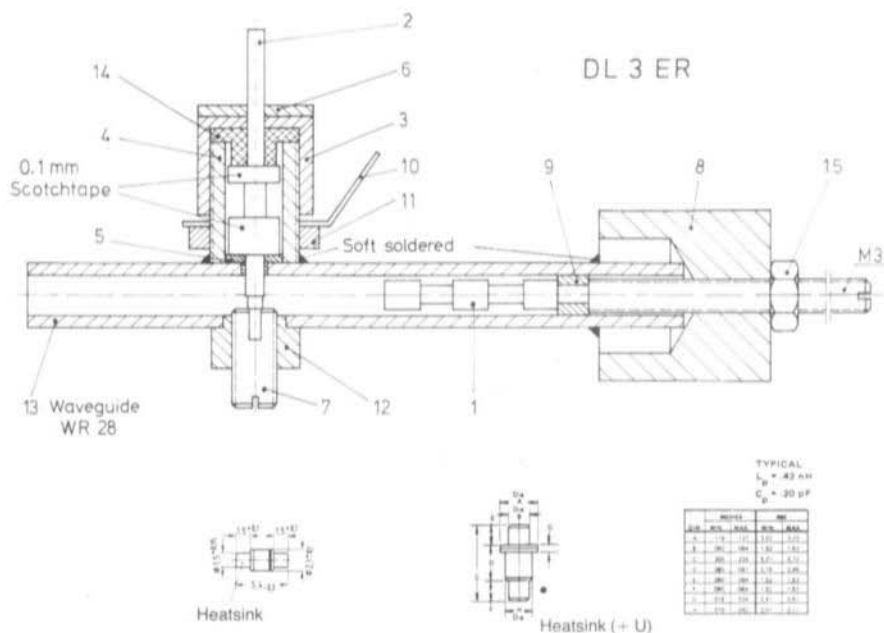
Fig. 1:   A contact-less, tunable 24 GHz, which can be used as Gunn oscillator or as detector/mixer according ti the semiconductor used.
Dimensions below left: Schottky diode; below right: Gunn element
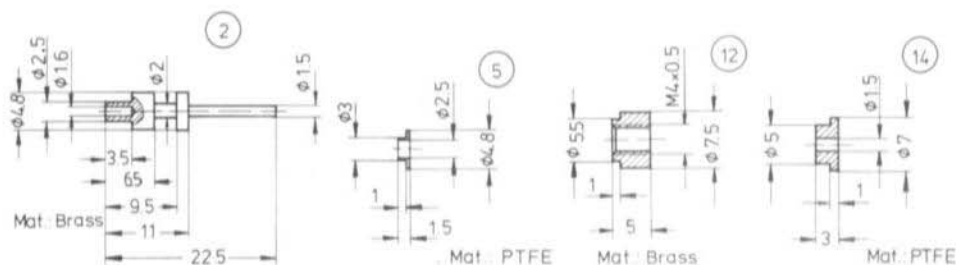


Fig. 2:   A few parts for the construction shown in Figure 1; other parts see parts list.

Parts 4 and 12 are fixed and soldered together paying attention that the holes are exactly oppposite to one another. For this reason, they should be drilled together previously using a 2 mm drill. Afterwards, it is possible to drill the planned holes of the correct diameter.

A centering tool should be made out of PTFE for part 4, which is then removed after soldering. A solder with a low melting temperature is required for this soldering process, and it is ad-

| Part | Designation, Material, Dimensions | Notes |
|------|-----------------------------------|-------|
| 1 | Tuning-choke system | as described in (2) |
| 2 | Choke for diode connection | see Fig. 2 |
| 3 | Bicycle valve nut | as described in (1) |
| 4 | Bicycle valve shaft, 12 mm long, inner diameter 5 mm | |
| 5 | PTFE bushing | see Fig. 2 |
| 6 | Isolating disk made from 1 mm thick PTFE, outer dia. 9 mm, hole 1.5 mm | without drawing |
| 7 | Diode screw from copper or brass M 4 x 0.5; 8 mm long, centered hole 1.6 mm dia. and approx. 5 mm deep | see Fig. 1 |
| 8 | Mount for tuning choke | as described in (2) |
| 9 | PTFE spacing ring | as described in (2) |
| 10 | Solder tag with 7 mm hole | |
| 11 | Nut from bicycle valve | |
| 12 | Threaded copper or brass bushing | see Fig. 2 |
| 13 | Waveguide WR 28 (R 320), approx. 55 mm long, with three-screw matching approx. 70 mm long | The length dimensions remain unchanged when using waveguide WR 42 (R 220) |
| 14 | PTFE bushing | see Fig. 2 |
| 15 | Counter nut M 3 | |

visable for the flange soldering joints to be protected against too much heat by using a wet paper handkerchief. The soldering process is made most favorably using a butane gas flame, and carrying out the soldering process with a relatively small electric soldering iron whose tip has also been heated additionally by the flame.

The soldering of part 8 to the flange is less critical; parts 4, 12, and the flange should, however, be covered by wet paper handkerchiefs as a cautionary measure. The same solder as used for soldering parts 4 and 12 should also be used here, and the same measures applied.

The assembly is made as shown in Figure 1. The connection choke for the diode, or Gunn element is now insulated with a layer of Sellotape. When using the module as Gunn oscilla-

tor, the required attenuator link should be soldered between part 2 and the ground solder tag to avoid parasitic oscillations: this is 22 nF in series with approximately 100 $\Omega$. In some constructions, it is sufficient to use the 22 nF capacitor on its own, with others it is necessary for a further 10 to 50 $\mu$F to be connected in parallel in order to suppress oscillation in the lower frequency range. This should be established experimentally and checked with the aid of an oscilloscope or TV-receiver.

The tuning choke is now inserted from the open side of the waveguide. The counter-sunk cone of approximately 120° allows it to be centered and fixed so that it is possible to insert a watch-maker's screwdriver and to place the threaded bolt into the associated hole after depressing the shaft of the choke.

## OPERATION AND RESULTS

The diode, or Gunn element should be inserted carefully in order to avoid a mechanical destruction of the component. The tuning with the aid of the choke system is very clear. In the case of resonators of this type using the $H_{10}$-wave, the waveguide chamber between semiconductor element and choke determines the frequency. The overall Q of this waveguide resonator determines the tuning width of the detector/mixer.

If a fine tuning is required, it can be made by inserting a metal screw — better PTFE — at a position of maximum electrical field strength. Such a position is approximately halfway between the semicondcutor element and the choke, as well as in the center of the wide side of the waveguide. The tuning slope can be decreased by taking the tuning screw from the center of the waveguide and placing it more towards the edge.

When used as a Gunn oscillator, the module supplies an output power of approximately 10 to 50 mW according to the Gunn element. This is obtained with the most favorable heat dissipation, and matching.

When used as a detector, (e.g. when using a Siemens Schottky diode type BAT 14-121) the module can be used well in conjunction with the frequency meter described in (3), as well as for simple radiation pattern measurements on antennas. In order to increase the sensitivity, it is possible to add a simple horn antenna having a gain of approximately 15 dB.

The author has also used this module as a receive mixer successfully. The absolute noise figure is not known, since only an uncalibrated noise source was available. However, this allowed comparison measurements to be made. These measurements showed that when using the described module with a low-noise Schottky diode of the BAT 14-series, approximately the same sensitivity values were obtained as were exhibited by straight-through mixers equipped with 1N26 diodes.

Of course, the attenuator link to avoid parasitic oscillation of the Gunn oscillator must be removed for such applications, since this would otherwise short-circuit the IF-path.

## HEAT PROBLEMS

When using this module as a Gunn oscillator, it should be mentioned that the heat dissipation, when using the described construction under continuous operation, could cause problems. Even low-power elements such as the MA-49628 operate at a voltage of typically 5 V with currents of 100 to 200 mA. At the low efficiency of only 2 to 5 %, a power dissipation of 0.5 to 1 W results which must be dissipated. For this reason, the good heat conductivity of copper should be used whenever possible. Especially when operating this module with higher power Gunn elements, it is advisable to provide a conventional black-coloured heat sink, or to use a copper block as heat sink. Of course, it is possible to use both.

All parts that become noticeably warmer than their environment should be made black so that they can radiate the excessive heat. Since a silver-plated surface can hardly dissipate heat, one should only silver-plate the surfaces carrying RF-current in the inside of the module.

All these measures will be useless if the heat transition from semiconductor element to mounting screw is poor, because the hole is too large. A good fit, and possibly a little heat-conductive paste are required here. Since heat dissipates itself only very slowly (in brass much slower than in copper), the semiconductor crystal can have already exceeded the critical temperature of 250° before a temperature

increase can be felt on the heat sink. Feeling is just not sufficient when trying to solve heating problems; one must study especially the transitions having a low surface area carefully to see whether they can conduct heat. To clarify the situation, it should be noted that the heat load of the transition crystal/case is approximately 5 W/mm² in the case of low-power Gunn elements ! In the case of the mentioned Gunn element, approximately 0.5 to 1 W must be conducted via approximately 8 mm², if the whole surface of the anode is in direct heat contact in part 7. If only a part of the surface is in contact, the specific heat loading will be higher. Heat-conductive paste will not solve all problems encountered with bad fit; it must be used sensibly: The RF-contacts must remain free of heat-conductive paste due to the losses involved.

## REFERENCES

(1)  E. Schaefer, DL 3 ER:
     Coaxial SHF-Connectors Constructed
     from Bicycle Tire Valves
     VHF COMMUNICATIONS 13,
     Edition 1/1981, pages 36-37

(2)  E. Schaefer, DL 3 ER:
     Chokes for Contactless Tuning of
     Waveguide Modules
     VHF COMMUNICATIONS 13,
     Edition 2/1981, pages 105-107

(3)  E. Schaefer, DL 3 ER
     A Wavemeter for the Frequency Range
     23.5 to 24.5 GHz
     VHF COMMUNICATIONS 13,
     Edition 4/1981, pages 235-238

# GaAs FET Masthead Preamplifiers for 144 MHz and 432 MHz with PTT and RF-VOX Switching

Selective High-Power Masthead Amplifiers in weather-proof cast aluminium case complete with mast brackets. Power supply and PTT via coaxial cable from shack using RF/DC Splitter. Insertion loss typically 0.3 dB.

| Type | Noise fig. | Gain dB | Max.Power | Price |
|------|-----------|---------|-----------|-------|
| SMV 144 A | 0.9 dB | 15/20 | 800 W SSB | DM 275.00 |
| SMV 144 G | 0.6 dB | 15/20 | 800 W SSB | DM 345.00 |
| SMV 432 A | 1.0 dB | 15 | 500 W SSB | DM 275.00 |
| SMV 432 G | 0.8 dB | 15 | 500 W SSB | DM 345.00 |
| With RF-VOX· | | | | |
| SMV 144 V | 0.9 dB | 15 dB | 200 W SSB | DM 279.00 |

RF/DC splitters:
PTT ............................................................. DM 74.50
VOX ............................................................. DM 64.50

Dimensions 125 x 80 x 28 mm (without brackets)
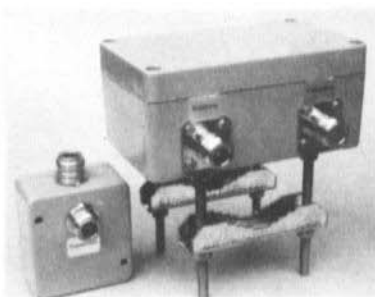
Lothar Damrow, DC 7 EP

# A Simple Electronic Fuse

Power transistors are the most expensive semiconductors of a transmitter, especially when high output powers are to be achieved at very high frequencies. They are always endangered when experimenting, whether it is during construction, alignment, repair, or when »only« trying to optimize the output power. It is always advisable to provide an electronic fuse in the operating voltage line, whose actuation current is adjustable to the maximum permissible value.

Similar to the description given in (1), the author has constructed a positive-pole fuse that can be realized with a minimum of components and be matched to modern conditions, in other words, 12 V operation at high currents.

## DEMANDS AND SPECIFICATIONS

The circuit should operate as a two-pole, in other words in the same way as a conventional fuse.

It should have a large variation range of voltage and current, without having to change the components.

Only a very low residual current should flow after actuation.

The author's prototype exhibited the following specifications:

Switchable voltage: $U_{b\,max} = 20\,V$
Maximal permissible continuous current:
$$I_{b\,max} = 5\,A$$
Voltage drop across the fuse $U_{dr}$:
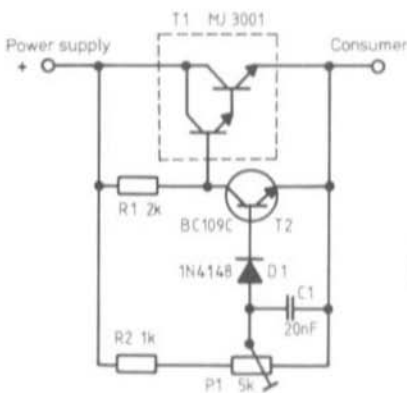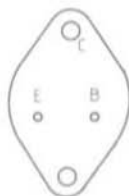


Fig. 1:
This electronic fuse can protect consumers up to 5 A

| $I_b$ (A) | $U_{dr}$ (Fig. 1) | $U_{dr}$ (Fig. 2) |
|-----------|-----------------|-----------------|
| 0.1 | 1.4 V | – |
| 1 | 1.6 V | 9.2 V |
| 2 | 1.9 V | 0.6 V |
| 5 | 3.5 V | 2.6 V |

Residual current after actuation (at $U_b$ = 12 V): 9 mA

## CIRCUIT DESCRIPTION

The circuit given in **Figure 1** is equipped with a power Darlington transistor in the main current circuit whose collector is connected to the positive pole of the power supply. The emitter represents the output to the consumer. Transistor T 2 is blocked, and thus high-impedance, which means that a voltage that is positive with respect to the emitter is fed via resistance R 1 to the base of T 1 and causes this to conduct.

Between collector and emitter of T 1, a consumer current having more or less voltage drop will be generated, and is also fed to the voltage divider comprising R 2 and P 1. A part of this is tapped off here and fed via diode D 1 to the base of T 2. As long as the tapped-off voltage is less than the sum of the threshold voltages of D 1 and the base emitter diode of T 2, T 2 will remain blocked and thus cause the fuse to conduct.

At a higher consumer current, and thus a higher voltage drop across T 1 or P 1, the tapped-off voltage will increase finally to such a value that T 2 will conduct. This will, in turn, cause T 1 to be blocked and the full operating voltage is now present across the fuse; only a very low residual current will flow, which will not endanger the consumer. This condition remains until either the power supply is switched off or the consumer is disconnected from the fuse. It should be mentioned that capacitor C 1 is provided to avoid an unwanted actuation of the fuse caused by steep current pulses. For safety reasons, its value should preferably be as low as possible.

## REDUCING THE VOLTAGE DROP

The voltage drop $U_{dr}$ cannot be neglected and is especially unwanted when the consumer does not draw a constant current, such as in the case of a SSB-amplifier or AF-power amplifier. A certain improvement can be achieved easily by providing a bias current. As can be seen in **Figure 2**, a load resistor of 100 Ω allows a bias current of 120 mA (at 12 V) to flow. This allows the voltage drop to be decreased by approximately 1.4 V, as can be seen in the previous table.
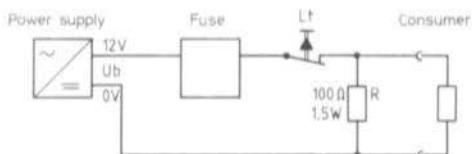


Fig. 2:
The voltage drop can be reduced by providing a slight extra load

The voltage drop across the electronic fuse can be completely eliminated if the stabilization is made subsequent to the electronic fuse as shown in **Figure 3**.

In this case, the electronic fuse with actuation button is installed in the power supply between rectifier / charge capacitor, and the stabilizer. However, it is necessary for the voltage at the charge capacitor to be at least 4 V higher than would be the case without fuse, if 5 A are flowing.
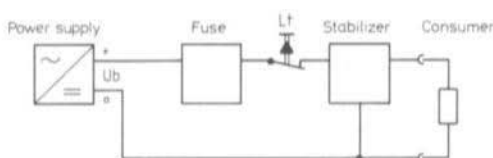


Fig. 3:
The voltage drop across the fuse can be completely eliminated when the fuse is installed between rectifier and stabilizer
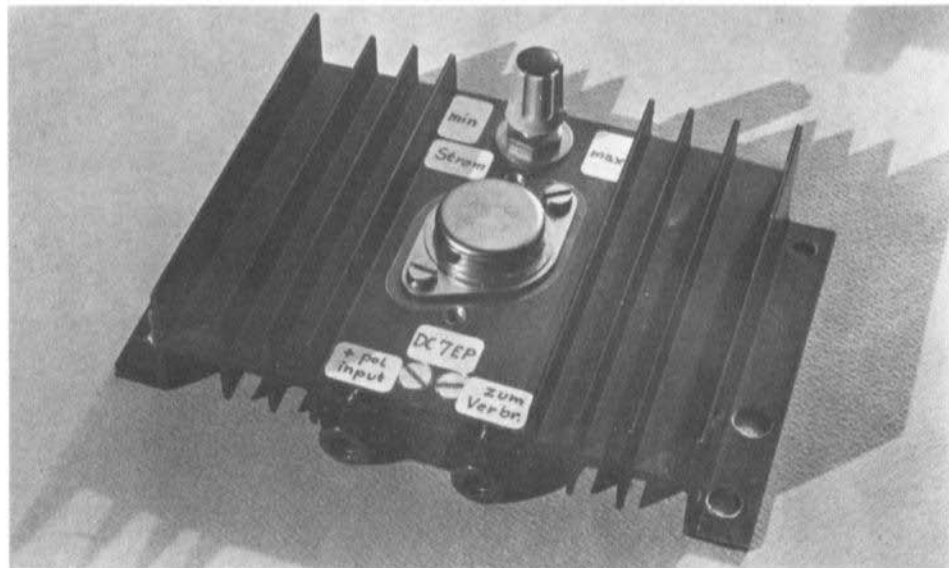
Fig. 4: Photograph of the author's prototype of a 5 A fuse built up on a heat sink

## MECHANICAL CONSTRUCTION

Due to the low number of components, no PC-board was developed for construction. As can be seen in **Figure 4**, the six parts can easily be installed on a heat sink of 115 x 75 x 25 mm.

If the fuse is to be installed in a power supply, and it is possible for transistor T 1 to be mounted on a suitable position on the case, it will probably not be necessary to provide a heat sink. The value of the maximum current is dependent on the size of the heat sink and on transistor T 1 itself. It is possible to operate the MJ 3001 up to approximately 2 A completely without heat sink.

Potentiometer P 1 is used for adjusting the required actuation current. Before using the fuse, it can be calibrated by connecting various load resistances. However, this can be difficult when a large number of different current values are required. It may then be advisable to replace the potentiometer by a switch having six to twelve positions and to use fixed resistors. The switch positions can then be marked with the measured actuation currents,

which would, of course, also be possible in conjunction with the potentiometer.

The components are not critical. The potentiometer should have a linear characteristic. Any modern silicon switching diode can be used for D 1. Transistor T 2 should have a high current gain, but does not need to have a metal case; the more modern BC 413 C, for example, should be just as suitable. The NPN-Darlington transistor MJ 3001 (or MJ 3000) cannot be replaced by a simple transistor such as type 2N 3055, even when it is enclosed in the same case. This is because only Darlington-transistors provide a sufficiently high current gain. Of course, one can use modern types in a plastic case instead of the old Motorola type. Suitable transistors are, for instance, BD 675 (Siemens), which are able to handle 45 V and 5 A.

## REFERENCES

R. Lentz, DL 3 WR:
A Simple Electronic Fuse
VHF COMMUNICATIONS 1, Edition 3/1969,
pages 174-178

*Leif Åsbrink, SM 5 BSZ*

# Dynamic Range of 2 m Transceivers

# Part 4: Modifications to the FT 221

A comparism of values measured on well-known commercial 2 m transceivers was given in part 1 (VHF COMMUNICATIONS 1/82) of this series of articles. Part 2, also in edition 1/82, gave a number of modifications to the TS 700, where part 3 (edition 2/82) gave modifications to the IC 211 and IC 245. The following part 4 will show how the FT 221 can be improved with respect to its dynamic range.

With respect to its noise sidebands, the FT 221 is one of the better stations even before modification. However, a few additional modifications can improve it considerably. The three stations given in **Figure 1** were used for experiments and lead to the described modifications.

Both the FT 221 and FT 225 can be equipped with a high-performance front-end board manufactured in the UK by Mutek. However, the high dynamic range of the Mutek board can only be utilized to the full if the VCO is modified.

Mutek specifies that an interfering signal at 144.300 MHz can be 115 dB over noise before an S9 signal at 144.400 MHz is degraded by 3 dB due to desensitization. This specification is hardly of interest, since a weak signal will be well in the noise due to the unwanted conversion with the noise sidebands of the VCO.

In its original state, the noise sidebands of the VCO are at − 90 dB. With an input signal of 115 dB above noise, the effective noise figure will be increased by 25 dB. This means that the same performance of adding the Mutek front-end could be obtained by inserting a 20 dB attenuator between antenna and receiver !

The two-tone dynamic range is more important (see the previous article). This is usually dependent on the purity of the local oscillator signal, or on the large-signal characteristics of the front-end. Little is achieved by improving the wrong circuit.

The situation is quite different when the VCO is modified. In this case the VCO noise can be reduced by appromately 20 dB at a spacing of 100 kHz which should directly improve the transmitter correspondingly (although the improvement is less in some cases as can be seen below). A Mutek or similar front-end will be required in addition in order to obtain a large improvement on the receiver.
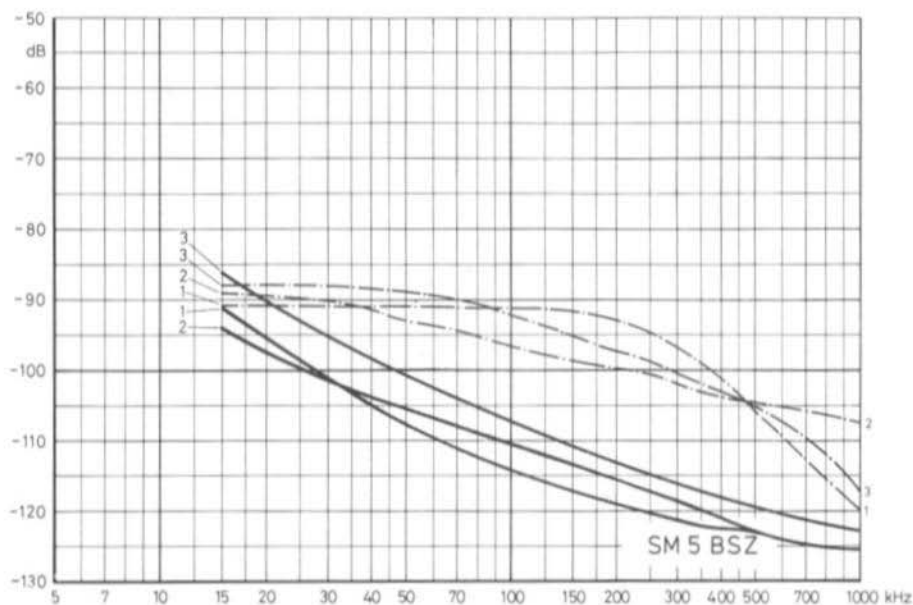
158

Fig. 1: Sideband noise as a function of frequency spacing from carrier.
Source: Three original FT 221 (dash/dotted lines), and after various modifications



Fig. 2: The effects of a good input circuit and improved VCO

The FT 221 annotated »1« in Figure 1 was measured in the receive mode. Curves A to C in **Figure 2** are those measured with the original VCO: whereas D to F show the results after the VCO modifications described in this article. Curves B and E were measured with the original front-end having a noise figure of 8 dB, which is typical for a Japanese transceiver. It would not be fair to make a direct comparison to such a transceiver equipped with a Mutek front-end having a noise figure of less than 2 dB (see curves A and D).

If a good preamplifier having a gain of about 15 dB is added to the original front-end, this will provide a performance similar to curves C and F. In this case, the noise figure would be the same as with the Mutek front-end, and a direct comparison between curves D and F shows the improvement that can be obtained by replacing the front-end in a station where the VCO has been modified.

A direct comparison between curves A and C shows that no improvement is obtained at moderate frequency spacings when using the original VCO, which underlines the above considerations.

In the case of the FT 221, the noise sidebands are mainly caused by noise from the phase-comparator (Note the unusually flat noise spectra of unmodified stations). This noise can be suppressed by changing the value of R 302 from 2.2 k$\Omega$ to 100 $\Omega$, and C 301 from 0.1 $\mu$F to 2.2 $\mu$F **(see Figure 3)**.

After carrying out this modification, performance is improved at frequency spacings in excess of 50 kHz, whereas the noise increases at lower frequency spacings. The source of sideband noise at this stage is the same as with unmodified IC 211 and IC 245 transceivers (see previous article in this series). The original fast response of the phase-locked loop in the FT 221 allowed the phase modulation of the VCO itself to be suppressed, however, this is no longer possible after changing the values of R 302 and C 301. This explains the degraded performance adjacent to the required frequency.

In order to obtain the performance shown in Fi-

gure 1, it is necessary to suppress the effects of the leakage currents by replacing R 323 and R 301 by RF-chokes. This was discussed in conjunction with the IC 211/IC 245. It is also necessary to suppress noise from the varicap diode D 306 of the bandswitch. This is achieved by cutting the conductor lane between R 322 and C 338 and bridging it with a 100 k$\Omega$ resistor. It should be noted that the original circuit diagram is not correct (for corrections see Fig.3). The 100 k$\Omega$ resistor and C 338 then form a low-pass filter. Also C 338 represents a low-impedance path for the noise components of the leakage current through the varicap diode. It should be mentioned that R 301 is usually replaced by an RF-choke in the factory.

The above changes cause the locking-in process to be 20 times slower. It is therefore necessary to change the value of C 342 from 0.1 $\mu$F to 0.68$\mu$F. Capacitor C 342 is in the circuit that detects an unlocked condition. It is necessary to increase the time constant, otherwise the transmitter could be switched on with the oscillator in unlocked condition.

One of the stations did not work after carrying out the above modifications. The reason for this was that the saw-tooth generator comprising C 301, R 302, R 306, and D 301 (unijunction transistor) no longer oscillated. The unijunction transistor was conducting continuously, with approximately 1 V at base 2 (connected to C 301). This problem was solved by increasing the emitter current by changing the value of C 303 from 10 $\mu$F to 100 $\mu$F and R 304 from 200 $\Omega$ to 100 $\Omega$. Replacing D 301 or inserting a resistor in the base 1 line, possibly in parallel with a large capacitor, are maybe a safer alternative.

Several FT 221 transceivers have been modified as above. The results shown in Figure 1 are representative, however, one source of sideband noise has still not been detected. It can be seen in station 3 of Figure 1, and the worst case known to the author is shown **Fig.4**, station A. This station was measured and modified at the 1981 Ånnaboda meeting. Unfortunately there was no time to investigate the problem.
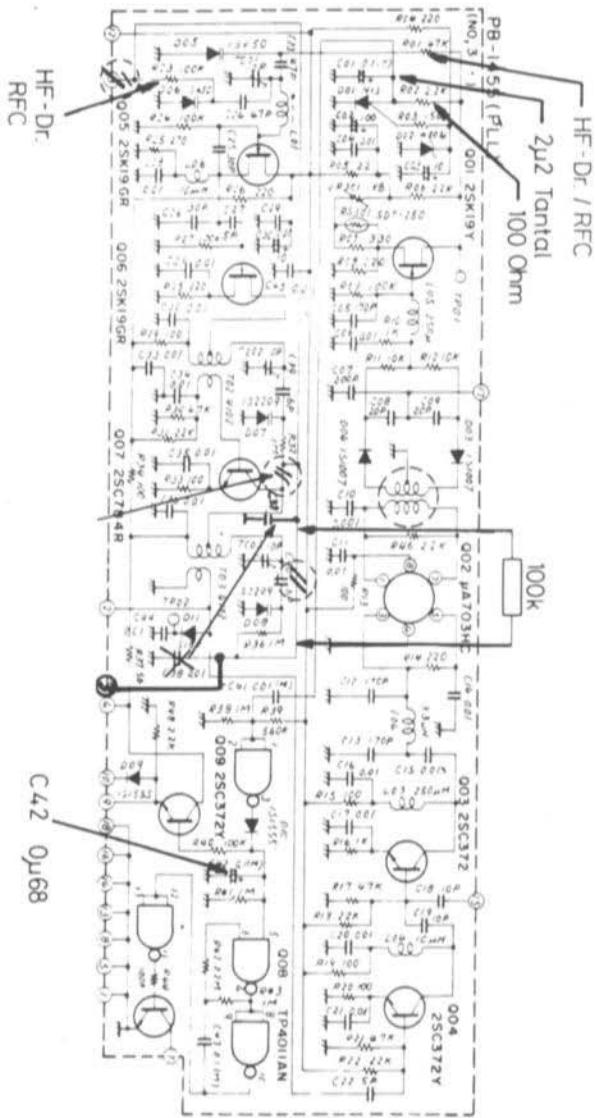
**Fig. 3:**
**Circuit extract with details**
**about parts to be modified**

Noise sidebands can be generated by amplitude modulation as a result of an insufficiently decoupled supply voltage to any amplifier or mixer in the transceiver.

A good example of this phenomenon is both the TS 700 described in the previous article, and station B given in Figure 4, which was modified according to a description where a potentiometer was connected in series with the emitter resistor R 512 of an amplifier to allow adjustment of the power output. Noise sidebands increase considerably when the power is decreased in this manner. The additional noise is probably caused by an increased sensitivity to AM of Q 503 as the current through this decreased. This can be suppressed by decoupling the supply voltage using a capacitor having a few μF. Station B was measured in Ånnaboda, however, before the problems could be studied in detail the station became defective due to a short-circuit that destroyed one of the driver transistors. The author still does not know whether the noise sidebands can be reduced at full power by providing an adequate decoupling of the supply voltage.
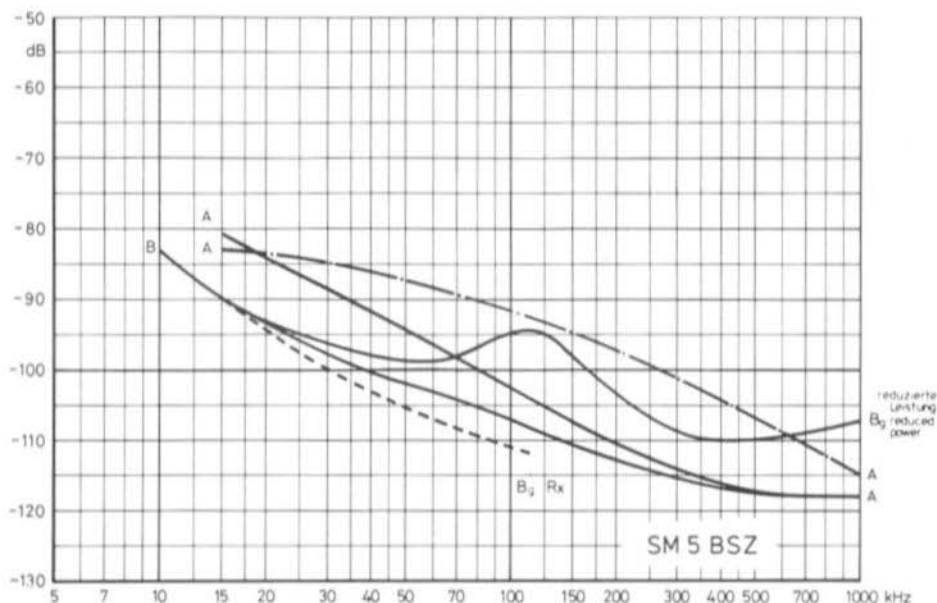
**Fig. 4:** A very poor example with unwanted AM due to poor bypassing, as well as effects caused by the emitter potentiometer used for output power reduction

When comparing the receiver performance of station B of Fig. 4, there is sure to be some AM noise in the transmitter even at full power output. This appears as additional noise at frequency spacings of approximately 100 kHz.

The time constant of the locking-in process is increased after carrying out the previous modifications, which is a disadvantage when using split-frequencies (FM-repeaters). This effect could be avoided using a few extra components (see previous article on IC 211/IC 245). However, since this effect was not considered to be important, no further experiments were made.

The keying of the FT 221 is very unsatisfactory as with most Japanese transceivers. Keying produces strong key-clicks. Despite this, the keying of many transmitters is not fast enough for high-speed meteor scatter work due to the poor design of the keying system.

A further article is to show how it is possible to get perfect keying without back-lash upto 1000 letters per minute, and with no key-clicks at a separation of 3 kHz. Both the principles and practical installation into the FT 221 are to be described.

Bernd Neubig, DK 1 AG

# The Optimum IF Selectivity for Coherent Telegraphy (CCW)

This article presents a further contribution to the subject of coherent telegraphy.

Coherent telegraphy allows a considerable reduction of the transmit and receive bandwidth. The main selectivity in the receiver (bandwidth less than 10 Hz) can only be achieved easily at AF-level (digital filter). As is known, these extremely small AF-bandwidths are only of limited value without sufficient pre-selectivity in the VHF and IF chains. This is because unwanted signals will pass through all stages up to AF-level and can cause desensitisation, inter-modulation, and unwanted control of the AGC-circuit.

This article is firstly to show how the minimum bandwidth of a IF-crystal filter is determined for telegraphy, and especially for CCW. Finally, various filter characteristics are compared with respect to their suitability. Part 2 of this article will then bring a proved circuit for home-construction.

## 1.
## LIMITING OF THE MINIMUM BANDWIDTH DUE TO THE CHARACTERISTICS OF THE CRYSTALS

Two important crystal parameters determine the lowest possible relative bandwidth of a crystal filter: The Q of the crystal, and the temperature response of the crystal frequency.

An insufficiently hig Q of the crystal will cause a marked rounding of the passband curve, and reduces the slope. Furthermore, it will increase the insertion loss of the filter (Figure 1).

A basic rule is that the crystal Q ($Q_q$) is at least 5 to 10 times the inverse value of the relative bandwidth $b_3/f_0$:

$$Q_p \geq 5 \text{ to } 10 \times \frac{f_0}{b_3}$$

At a center frequency of 9 MHz, filter crystals have Q-values of approximately 120 000 to 150 000 which corresponds to a minimum bandwidth of 300 to 600 Hz. When using special crystal designs (e.g. overtone crystals), it is possible to increase the Q to 500 000 and more, which results in narrower filters.
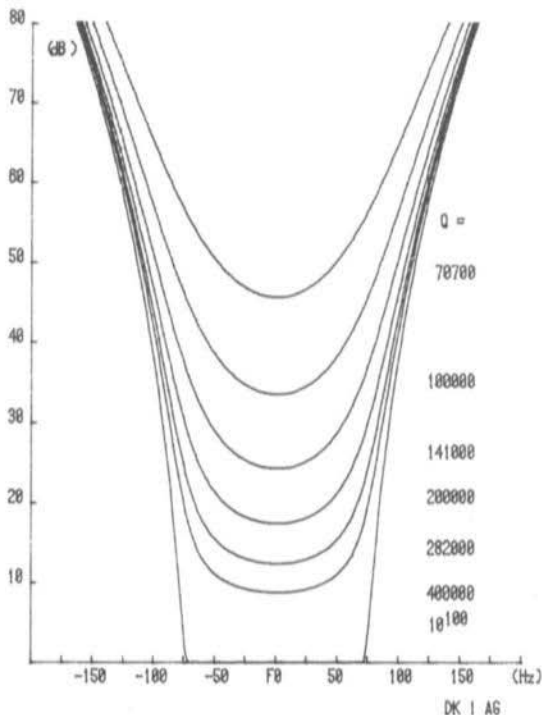
Fig. 1:
Filter curves as a function
of Q of the crystals used

The temperature response of common filter crystals amounts, for example, in a temperature range of 0°C to 50°C, to ± 5 to ± 10 ppm; at a frequency of 9 MHz, this results in ± 45 to ± 90 Hz that the crystals can run, sometimes in opposite directions (1).

For this reason, the temperature response of the crystals used in very narrow crystal filters must be operated at their theoretical limits, which is in the order of ± 1.0 to 1.5 ppm (9 to 15 Hz) in our example. For higher demands, such filters are often placed in crystal ovens.

Another alternative would be to select a further lower intermediate frequency below 1 MHz. Crystals in this range have, it is true, a somewhat lower Q, however, the relative bandwidth is lower for a certain bandwidth and thus the demands on the crystals are lower. On the other hand, good crystals are expensive in this frequency range, and are also larger. The main disadvantage is, however, the additional conversion.

## 2.
## LIMITING OF THE MINIMUM BANDWIDTH DUE TO THE PULSE BEHAVIOUR

Every CW-man will know that narrow-band filters tend to ring at higher transmission speeds. This means that the »clean« CW-signal from the transmitter is distorted: Rise and fall slopes are flatter, and overshoots will appear.

The frequency spectrum of a periodically keyed HF-carrier possesses a number of lines spaced at multiples of the keying frequency in addition to the carrier frequency. In the case of CW-transmissions, these lines will form a virtually continuous spectrum. If the group delay (which is the delay time required for the envelope of the CW-signal to pass from the filter input to output) is not equal for all spectrum components, this will mean that these components will arrive at the output at different times. They
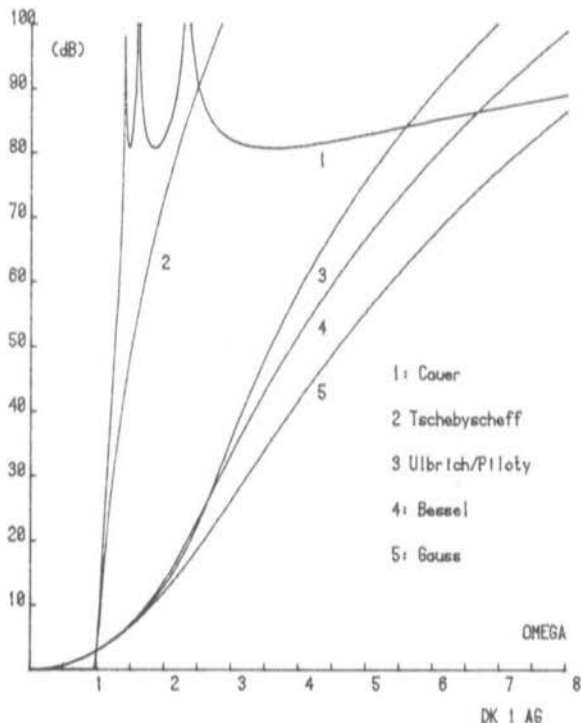
Fig. 2:
Comparison of the passband
curves of five common filter
characteristics

1: Cauer

2 Tschebyscheff

3 Ulbrich/Piloty

4: Bessel

5: Gauss

will then be combined at the output and result in a distorted waveform.

With normal filters, the group delay is at a minimum in the center of the passband range, and increases to a multiple of this at the edge of the passband range (see Section 3). The narrower the filter, the greater the effect of these group delay distortions, since they distort the low-order spectrum components, which have the greatest effect on the waveform.

# 3.
# PULSE BEHAVIOUR AND SELECTIVITY OF VARIOUS TYPES OF FILTER

An ideal CW-filter would be a filter having a most constant group delay over the whole passband range (2), as well as a bandpass characteristic that was as narrow as possible and possessed the steepest possible slopes.

Unfortunately, these two demands cannot be achieved at the same time: A filter with a good pulse behaviour will have a poor selectivity, and a steep filter will have a poor pulse behaviour; Both characteristics are connected together mathematically, and every practical solution represents a compromise between both demands.

This is now to be discussed in conjunction with various, common filter characteristics. An 8-- pole filter with a bandwidth of 150 Hz is to be assumed in the examples. The appropriate bandpass curves are given in **Figure 2**, whereas **Figure 3a and 3b** show the group delay in the passband range, and **Figure 4** the pulse behaviour of these filters.

Fig. 3a:
Group delay of Cauer
and Chebishev-filters
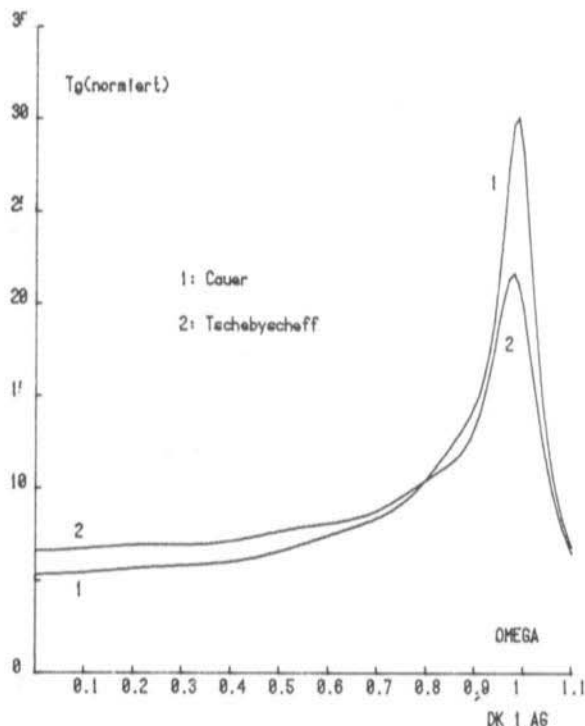
All curves are given in standardized form. In the case of the frequency axis, $\Omega = 0$ corresponds to the center frequency, and $\Omega = \pm 1$ to the 3 dB points on the filter characteristics. The axis is therefore calibrated in multiples of half the 3 dB bandwidth.

The group delay $\tau_g$ is also standardized as $T_g$: the group delay $\tau_g$ (in sec) is obtained for a certain filter having a 3 dB bandwidth $b_3$ (in Hz) from the following equation:

$$\tau_g = \frac{T_g}{\pi \times b_3}$$

The pulse behaviour is the shape of the output signal (i.e. the demodulated envelope), which results when the carrier $f_0$ at the input having an amplitude »1« is suddenly (ideally square-wave«) switched on.

The time axis is also given in standardized

units T and can be recalculated into seconds using the following equation:

$$t = \frac{T}{\pi \times b_3}$$

Table 1 shows a list of the most importants data. The first four columns give the stopband-width in $\Omega$-units (shape factor). The following columns contain the most important data about the standardized group delay: The value at the center frequency $T_{go}$, the maximum value, the value at the 3-dB-points, and the point at which the group delay has fallen off by 10 % with respect to $T_{go}$.

Table 1

The lowest part of the Table describes the pulse behaviour: The overshoot in % and the (standardized) times after which 50 % and 90 % of the final amplitude »1« is achieved.

**Fig. 3b:**
Group delay of Ulbrich/Piloty, Bessel, and Gauss filters

Tg(normiert)

3: Ulbrich/Piloty

4: Bessel

5: Gauss

OMEGA

DK 1 AG
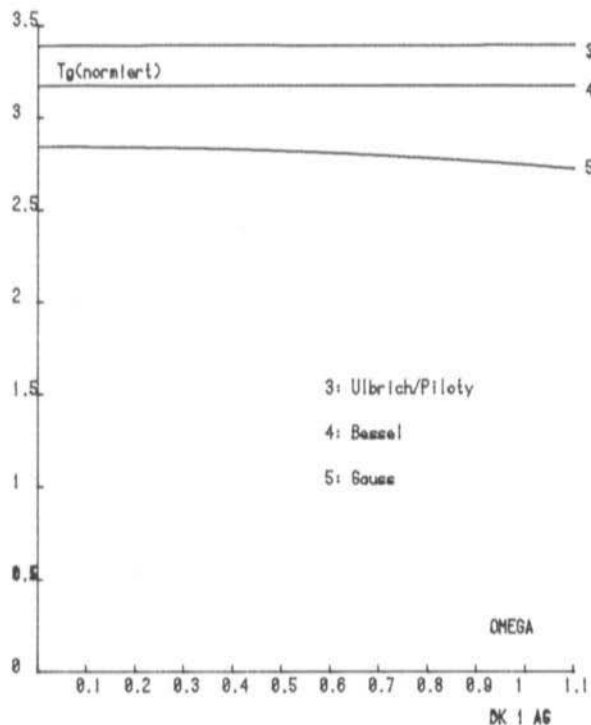
| Characteristics | Type of Filter Cauer C 0815b-45° | Tschebyscheff C 0815b-T | Gauß 8 Pol | Bessel 8 Pol | Ulbrich/Piloty d = 0,01 / 8 Pol |
|---|---|---|---|---|---|
| Selectivity | | | | | |
| $\Omega$  (20 dB) | 1,085 | 1,136 | 2,60 | 2,35 | 2,40 |
| $\Omega$  (40 dB) | 1,201 | 1,362 | 3,90 | 3,34 | 3,17 |
| $\Omega$  (60 dB) | 1,314 | 1,700 | 5,38 | 4,53 | 4,07 |
| $\Omega$  (80 dB) | 1,380 | 1,884 | 7,28 | 6,08 | 5,30 |
| Group delay | | | | | |
| $T_{go}$  ($\Omega = 0$) | 5,359 | 6,630 | 2,842 | 3,174 | 3,389 |
| $T_{max}$ | 30,117 | 21,600 | — | — | — |
| $T_{g\,3\,dB}$  ($\Omega = 1$) | 28,185 | 19,737 | 2,741 | 3,174 | 3,394 |
| (10 %) | — | — | 1,63 | 2,07 | 2,51 |
| Pulse behaviour | | | | | |
| Overshoot | 19,82 % | 18,49 % | 0 | 0,45 % | 0,44 % |
| T  (50 %) | 5,9 | 7,1 | 2,67 | 3,04 | 3,26 |
| T  (90 %) | 7,4 | 8,5 | 3,83 | 4,16 | 4,36 |

Table 1: Selectivity, group delay, and pulse behaviour of various filter characteristics
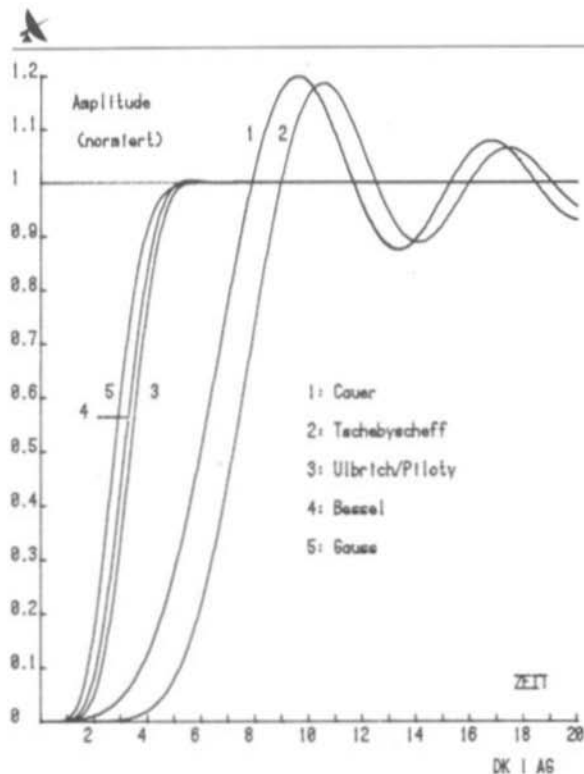
Fig. 4:
Comparison of the pulse
behaviour of the pre-
viously mentioned five
types of filters

## 3.1.
## CHEBISHEV-FILTER

This is the most commonly used filter charac-
teristic. Most of the CW-filters on the market
are of this type. Chebishev-filters have a very
good selectivity, with steep slopes, where a
slight (the theoretic !) ripple is permissible in
the flat top of the passband range. In our ex-
ample, the ripple is 0.0988 dB (≙ 15 % reflec-
tion). The actual ripple is usually higher due to
component and alignment tolerances.

In the stopband range, the attenuation will con-
tinue to increase. In the given case, the shape
factor amounts to (60 dB : 3 dB) = 1.7, with a
60 dB bandwidth of 425 Hz; the designation of
this filter is: C 0815b-T (see[5]). The group de-
lay increases, however, steeply at the edge of
the passband range and achieves a maximum
of 45.8 ms in our example with respect to 14.1
ms at the center frequency. When one obser-
ves the pulse behaviour, one will see that the
filter reacts after a very large delay: 90 % of

the final amplitude is achieved only after 18.0
ms. Furthermore, it overshoots greatly by
18.5 % and the oscillation is reduced slowly
what generates the well-known ringing effect.
When one considers that the dotlength is only
40 ms (4) at a speed of 150 letters per minute
and that with RTTY at a speed of 45.45 (100)
Baud the unit length amounts to 22 (10) ms,
the resulting output signal can be assumed !

If the (theoretical) ripple is reduced to zero,
one will obtain the so-called potential or Butter-
worth-filters. However, these are not to be
dealt with here, since they do not bring any im-
provement of the pulse behaviour.

## 3.2.
## CAUER-FILTER

In order to increase the slope steepness
further, additional attenuation poles are gene-
rated in the stopband range with Cauer-Filters

168

(»elliptical filters«). In the example, the first pole position was set at $\Omega = 1.403$, and the ripple in the passband range was selected to be the same as that of a Chebishev-filter (filter terminology: C 0815b-45°, see [5]). The resulting shape factor amounts to 1.31, which means that the 60 dB bandwidth amounts to only 328 Hz !

The group delay is similar to that of the Chebishev-filter, however, with a higher overshoot of 11.3 ms (center frequency) to 63.8 ms at the limit. The pulse behaviour is even worse: it is true that the pulse appears somewhat faster (90 % after 15.7 ms) however, the overshoots are stronger (19.8 %) and take more time to decay. The improved selectivity is obtained at the cost of the pulse behaviour.

## 3.3.
## GAUSS-FILTER

With this type of filter, the passband curve approximates the well-known Gaussian distribution curve — the larger the number of poles, the better —. Gauss-filters have an ideal pulse behaviour with very fast rise time (90 % after 8.13 ms) and without overshoot. However, the selectivity is very poor: 60 dB are achieved firstly at 5.38 times the bandwidth (1345 Hz) !

The group delay sinks very little at the 3-dB-point (6).

## 3.4.
## BESSEL-FILTER

In the case of Bessel-filters, (also called Thomson-filters), the group delay is optimized to have the best flat characteristic (7). In our example, it amounts to 6.73 ms over the whole passband range. It falls off by 10 % first at 2.07 times the bandwidth. The pulse behaviour has only a very slight overshoot of 0.45 %, which ceases immediately; the rise time is slightly

slower (90 % after 8.83 ms) as was the case with the Gauss-filter.

However, the selectivity is much better: The shape-factor 60 dB : 3 dB is 4.53, corresponding to a bandwidth of 1130 Hz.

## 3.5.
## ULBRICH/PILOTY-FILTER

This filter is also called an »Equiripple-Phaselinear Filter«, and is a further development of the Bessel-filter by allowing the group delay to have a certain ripple (as was the case for the attenuation of the Chebishev-filter). This means that the group delay is constant over a far wider range, and the selectivity is also improved (8). In our example (standardized ripple 0.01), the 60 dB : 3 dB shape factor amounts to 4.07 (1018 Hz), the group delay amounts to 7.20 ms, and falls off by 10 % firstly after 2.5 times the bandwidth.

The pulse behaviour is very similar to that of the Bessel-filter: Overshoot 0.44 %, 90 % of the amplitude is achieved after 9.25 ms.

In addition to these filter characteristics, there are any number of further compromises, which would be far to extensive to be described in this article. To summarize, one can say that the cause of »ringing« of a filter is usually not that the bandwidth is too low, but more that the filter characteristic is not optimized.

## 4.
## HOME-CONSTRUCTION OF A CCW CRYSTAL FILTER

The previously discussed 8-pole filter cannot be achieved in home construction, since the limits are in the order of a 4-pole filter. In order to still achieve a sufficient selectivity, two four-pole filters of the Ulbrich/Piloty type are to be connected in series using an intermediate
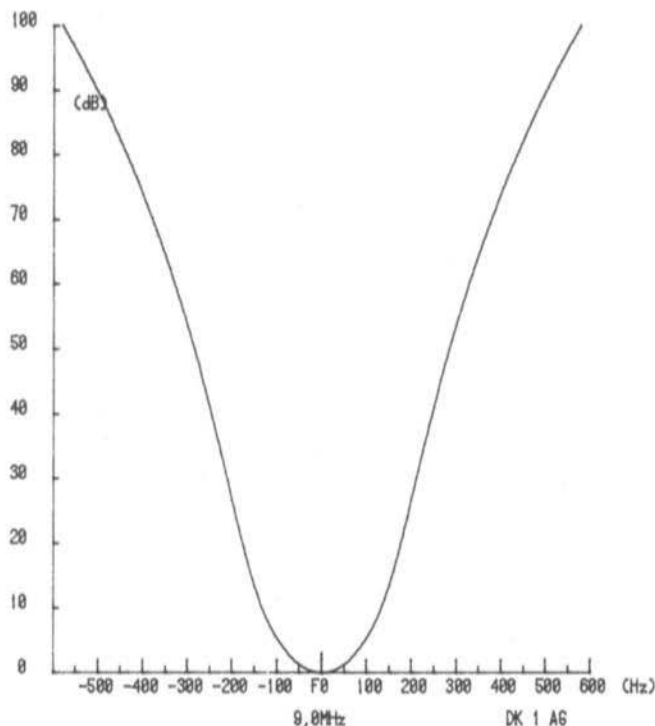
100
90
80
70
60
50
40
30
20
10
0
(dB)
-500
-400
-300
-200
-100
F0
100
200
300
400
500
600
(Hz)
9,0MHz
DK 1 AG

**Fig. 5a:**
**Passband curve of the home-made filters described in part 2**

large-signal amplifier stage as buffer. The amplifier stage has two tasks: Firstly it is to provide both filters with a pure ohmic termination – which would not be the case if they were connected directly in series: and secondly, it must compensate for the total insertion loss of the two filters of approximately 12 dB.

When using this circuit, one achieves virtually the same selectivity, with only a slight deterioration of the pulse behaviour when compared with an 8-pole filter.

Part 2 of this article will describe a 9 MHz-filter with a bandwidth of 150 Hz at – 3 dB (measured using both filters). In order to recalculate this filter for other center frequencies it is necessary to know the crystal equivalent data that can be realized (especially the dynamic capacitance $C_1$ or inductivity $L_1$) (9).

**Figure 5** shows the theoretical selectivity curves and the appropriate group delay. The practical construction and the measurement will be carried out by F. Krug, DJ 3 RV as soon as the special crystals are received. This will be followed by a constructional article.

## REFERENCES AND FOOT NOTES

(1) B. Neubig, DK 1 AG:
Design of Crystal Oscillator Circuits
VHF COMMUNICATIONS 11,
Edition 3/1979, pages 174-190
Concluding part 2:
VHF COMMUNICATIONS 11,
Edition 4/1979, pages 223-237

(2) Exactly speaking, it is not sufficient to have a constant group delay to obtain an ideal pulse behaviour, but it is necessary, at the same time, to have a rounded shape of the passband curve. This is the so-called Gibbs phenomena: The Gauss filter will have a better pulse behaviour than the Bessel-filter although its group delay is not so constant
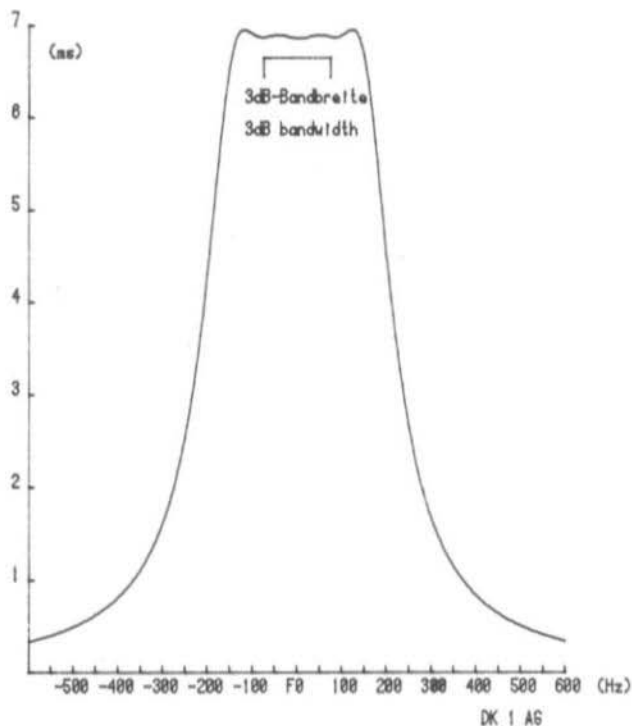
(3) Belevitch, Vitold:
Chebishev-Filters and Amplifier Net-
works – Wireless Engineer
(Apr. 1952), pages 106-110

(4) D. Burberg, DJ 2 YE:
Geschwindigkeitsbestimmung bei
elektronischen Tasten
CQ-DL Edition 8/1981, page 384

(5) R. Saal:
Handbuch zum Filterentwurf
AEG-Telefunken 1979

(6) M. Dishal:
Gaussian-Response Filter Design;
Electrical Communication, Vol.36 No.1
(1959), pages 3-26

(7) W. E. Thomson:
Delay Networks Having Maximally-Flat
Frequency Characteristics.
Proc. IEEE, Vol. 96 (1949), pt.3,
pages 487-490

W. E. Thomson:
Networks with Maximally-Flat Delay
Wireless Engineer, (October 1952),
pages 256-263

(8) E. Ulbrich, H. Piloty:
Über den Entwurf von Allpässen, Tief-
pässen und Bandpässen mit einer im
Chebishev-schen Sinne approximierten
konstanten Gruppenlaufzeit.
Archiv El. Übertragung, Volume 14
(1960), H.10, pages 451-467

(9) U. L. Rohde, DJ 2 LR, published a com-
puter program in QST, May 1981, pages
18-23: »Crystal Filter Design with Small
Computers«; however this article pos-
sesses a large number of errors, and one
cannot recommend its use. The calcula-
tion of the described filter is also made
with somewhat different methods. On re-
quest, the author DK 1 AG is prepared to
provide further assistance.

*Friedrich Krug, DJ 3 RV*

# A Versatile IF-Module Suitable for 2 m Receivers, or as an IF-Module for the SHF-Bands

# Part 3: Controlled IF-Amplifier, Notch Filter, Demodulators, BFO, and AF-Amplifier

**The following article is the final part of a series describing the individual circuits and the measured values that can be obtained. The selection of the circuit to be used is discussed, as well as one or other method, which were not used in the final design. This extensive discussion of the circuit is provided to assist those readers who have sufficient experience and do not wish to construct the whole receiver. This will allow them to carry out their own experiments based on these circuits. For those readers wishing to construct the complete IF-module, full constructional details including the complete circuit diagram and PC-board layout will be described in one of the next editions of VHF COMMUNICATIONS.**

## 3.3.
## CONTROLLED IF-AMPLIFIER WITH S-METER

The task of the second module (see **Figure 4**

in Part 2) is to amplify the IF-signal to a sufficient level for it to be demodulated. Demodulators will operate most favorably when the mean value of the input signal remains virtually constant and is within the dynamic range of the demodulator so that it is not overdriven by the input signal. In order to achieve this, the IF-amplifier must satisfy three important characteristics:

**A.** A very high, low-noise gain, which ensures that the weakest received signals will provide a sufficient level at the demodulator so that they can be demodulated without deteriorating the signal-to-noise ratio.

**B.** An AGC-range of at least equal to the dynamic range of 100 dB given in section 3.1.1.

**C.** A non-limiting input level range of $\geqq$ 100 dB; it must be taken into consideration that the module equipped with the crystal filters will have already amplified the signal by approximately 20 dB. This means that the amplifier must be able to process input voltages from 5 μV to 500 mV.
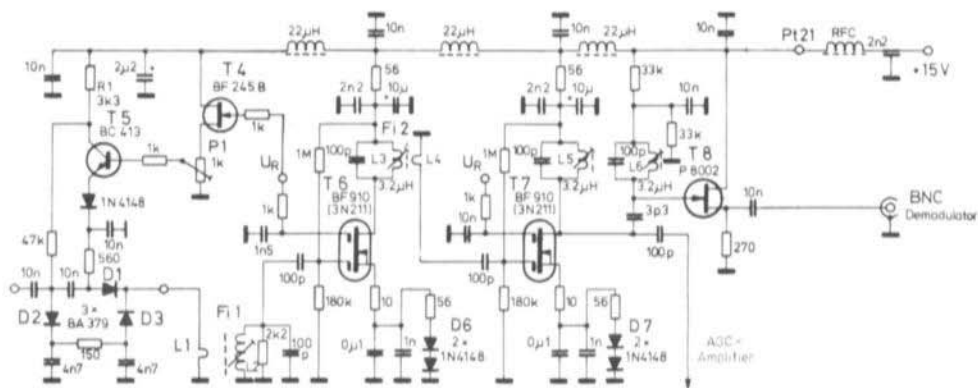
**Fig. 13: The controlled IF-amplifier with a large dynamic range and short control-time constants**

In order to ensure that the module can be connected without problems to the other modules, the input and output impedances are 50 $\Omega$, and the mean output level under controlled conditions is set at 10 mV across 50 $\Omega \triangleq -27$ dBm for the output to the demodulator module (for the IF-output to 25 mV across 50 $\Omega \triangleq -19$ dBm).

After taking the gain of the crystal filter module into consideration, the lowest input level will amount to 5 $\mu$V into 50 $\Omega \triangleq -93$ dBm. The non-load gain of the IF-amplifier should therefore not exceed

$$G_p = -27 \text{ dBm} - (-93 \text{ dBm}) = 66 \text{ dB}$$

otherwise the control circuit would be actuated by noise. Dual-gate FETs are used as amplifiers. These components are inexpensive, and it is assumed that they will be available for many years.

With respect to their technical characteristics, VHF-dual-gate FETs are virtually ideal. They have a high slope, which means that a gain of approximately 40 dB per stage can be achieved; they also possess a low reaction which means that it is possible to construct a reliable circuit without neutralization; a low noise in

order to obtain a high signal-to-noise ratio and a large dynamic range of > 50 dB per stage. The only disadvantage is the previously mentioned low input dynamic range under controlled conditions. This can be improved by using an additional control with a PIN-diode in front of the first DG-FET as was recommended by DJ 1 SK in (16). In order to ensure that the input impedance is virtually independent of the control state, a PIN diode attenuator using a Pi-circuit is used.

The circuit diagram of the controlled IF-amplifier is given in **Figure 13**.

### 3.3.1. PIN Diode Attenuator

In its forward direction, the PIN-diode represents a resistance for frequencies f > 1 MHz, whose value can be controlled with the aid of the forward current.

With a high DC-current in forward direction, $I_F$, the RF-resistance of the diode will be small, whereas it will increase at a low $I_F$. The attenuator shown in Figure 13, is constructed using such PIN diodes in a Pi-circuit. The con-

trol voltage drives the current in the pass diode D 1 via the source follower T 4, or the emitter follower T 5. The voltage drop across R 1 caused by this current drives the current in diodes D 2 and D 3. If the current through D 1 decreases, the voltage drop across R 1 will also decrease, thus increasing the current in D 2 and D 3. The resistance of diode D 1 will thus increase and the resistance values of D 2 and D 3 will be reduced. This means that the attenuation of the Pi-circuit will therefore increase. The calculation of the attenuator was made according to information given in (17).

The circuit should be designed so that the input impedance $Z_{in}$ is 50 $\Omega$ $\pm$ 10 % throughout the whole dynamic range. It is important that the attenuator is terminated with 50 $\Omega$ at the output. The attenuation characteristic of the PIN diode in the overall circuit as a function of the control voltage is given in **Figure 14**. For higher input levels, the diodes will be controlled by the RF-signal, which decreases the attenuation and will cause the signal to be distorted.

## 3.3.2. Controlled Amplifier

As has been previously mentioned, dual-gate FETs are to be used in the amplifier. The required dynamic range and the control time constants determine the design of the circuit. The gain of $G_p \leqq 66$ dB can be achieved using a two-stage amplifier, as can be the required dynamic range of 100 dB.

The amplifier is built up using two DG-FETs BF 910 in a common-source circuit as shown in Figure 13. The design criteria for these FETs were given by DJ 1 SK in (18). Unfortunately, the most favorable input impedance for minimum noise is not given in the data sheet of the BF 910. Noise figure measurements showed that this value must be in the order of 1 k$\Omega$.

The matching to this value has been realized using resonant circuits. The resonant circuit between the attenuator and T 6 has a turns-ratio of 1:5 and also guarantees the required 50 $\Omega$ termination for the PIN diode attenuator.
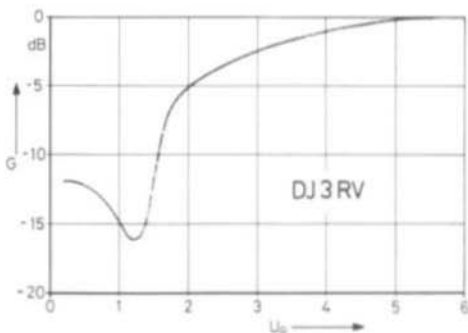


Fig. 14:
The attenuation characteristics of the PIN diode attenuator in the overall circuit shows the reduced attenuation at high input levels clearly
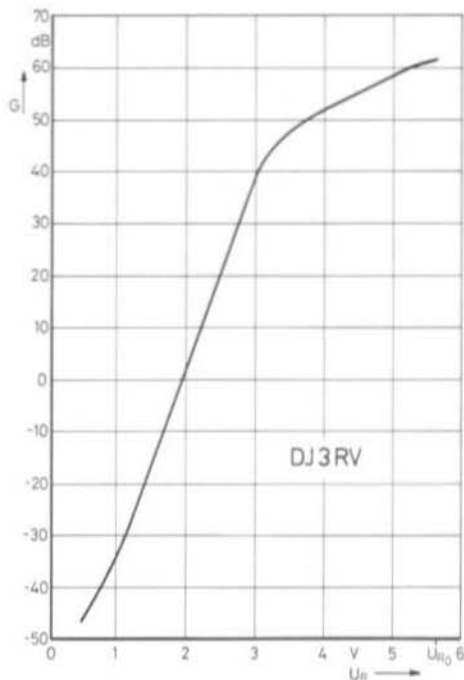


Fig. 15:
The gain of the controlled IF-amplifier as a function of the control voltage showing the two different ranges of the logarithmic characteristic

The coupling between T 6 and T 7 is achieved using a resonant circuit with a turns-ratio of 4:1.

The signal is amplified in T 7 and fed via a capacitively coupled bandpass filter and the source follower T 8 to the output for the demodulator module. The output impedance amounts to 50 $\Omega$ due to the use of the source follower. The input capacitance of the source follower is compensated for using the LC-circuit. This stage therefore has the tendency to self-oscillation under non-load conditions, which means that it should only be operated together with a real-load of approximately 50 $\Omega$.

The resonant circuits are relatively wideband so that the signal delay in the amplifier is short. With a suitable design of the time constants in the AGC-amplifier, it is possible to still control level change rates of 10 dB/µs. However, a considerable phase modulation of the signal will occur which leads to distortion during AM-demodulation when using synchronous demodulators, and during FM-demodulation when using a phase demodulator. This is especially valid when the level variations are caused by interfering signals. Due to the transcient behaviour of the crystal filter in the first module, the

level variation rate at the widest bandwidth is limited to max. 1.5 dB/µs, if the dynamic range is not exceeded. It should be mentioned that the first module, as well as the noise blanker designed by DJ 7 VY produce phase interference when strong interfering pulses are received. This is especially unpleasant when using modulation modes with which the information is transmitted by phase-shift keying, such as with coherent telegraphy (CCW).

The gain control of DG-FETs is made most easily by varying the voltage at gate 2. For maximum gain of the FET, the voltage between gate 2 and source $U_{G2S}$ should amount to 4 V. On decreasing voltage, the slope of the transistor will be reduced, and thus the gain.

A gain variation of approximately 50 dB per stage requires a voltage variation of 5 V at gate 2. In order to avoid negative control voltages, the source potential is increased by the value of the voltage drop across the diodes. This results in a control characteristic for the IF-amplifier as shown in **Figure 15**.

**Figure 16** shows the output voltage $U_{out}$ as a function of the input level. The control commences at an input voltage of 7 µV $\triangleq$ − 90 dBm, and maintains a virtually constant output
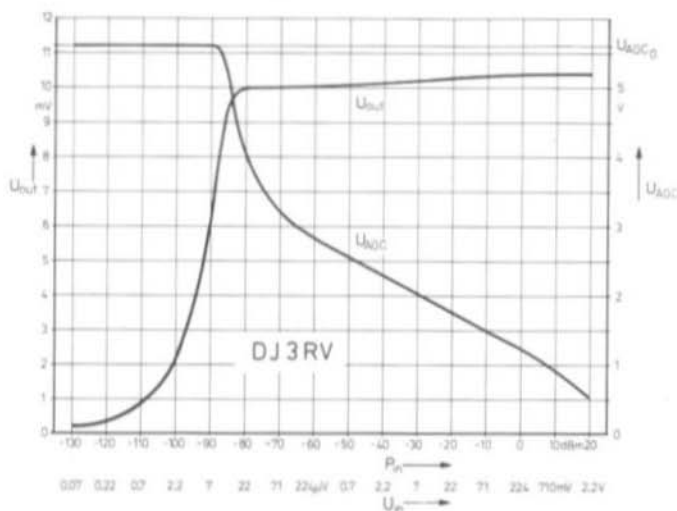


Fig. 16:
The output voltage $U_{out}$ and the control voltage $U_c$ as a function of the input power $P_{in}$ or the input voltage $U_{in}$ over a dynamic range of 150 dB .
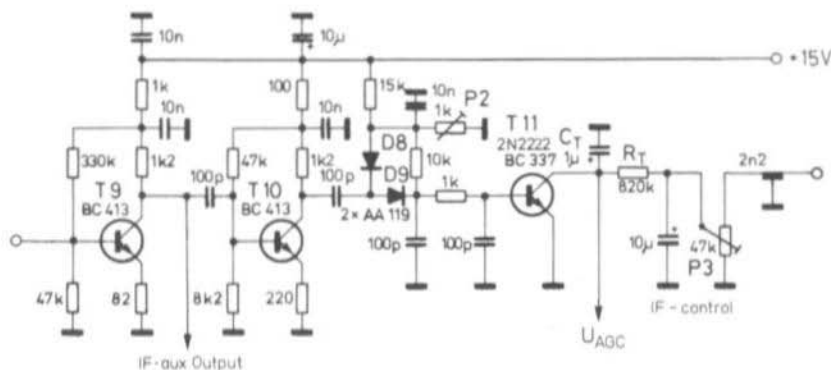
**Fig. 17:**
The control voltage generation having a very short rise time

voltage of 10 mV up to an input voltage of 2.2 V $\triangleq$ + 20 dBm. Distortions caused by limiting the modulation peaks commence at 500 mV. An AM-signal modulated by 30 % would then possess a distortion factor of approximately 3 %. This is a good value for amateur applications.

The noise figure is deteriorated by the PIN-diode attenuator, is, however, still only 6 dB, which means that it can be neglected in the overall concept. The noise power provided by the first module is much higher.

### 3.3.3. Control Voltage Generation

After setting a level of 10 mV at the demodulator output, a mean signal voltage of 25 mV will be present at the drain of T 7. This level is not sufficient for direct rectification and must therefore be amplified. The circuit of the control voltage amplifier and control voltage generator is shown in **Figure 17**. The signal voltage is amplified to a value of approximately 1 $V_{pp}$ in a two-stage amplifier. The first stage has a voltage gain of four times, and the second of three times. The IF-signal is coupled out after the first stage. The signal is then available with sufficient level at the IF-output connector for further processing.

After the second stage, the signal is then fed to the control voltage rectifier equipped with the

germanium diodes AA 119. The rectified signal voltage controls transistor T 11, which discharges capacitor $C_T$ to the required control voltage potential. The gain of the IF-amplifier will reduce together with the decreasing control voltage $U_{AGC}$ across capacitor $C_T$.

With the aid of the voltage divider comprising the 15 k$\Omega$ resistor and the 1 k$\Omega$ potentiometer, it is possible to vary the bias voltage at the base of T 11 so that the control voltage threshold and the output amplitude of 10 mV can be set at the output for the demodulator.

The maximum control voltage results when transistor T 11 is blocked. The switchable 4.7 k$\Omega$ potentiometer parallel to the zener diode can be used as »manual control« where the control is maintained at a greater level. This allows the highest control voltage, and the control threshold to be selected.

The dynamic control behaviour of the IF-amplifier must be matched to the different modulation modes, and an absolute value is very difficult to establish since it is very dependent on the personal requirements. Fundamentally speaking, the control should be actuated quickly so that the demodulator is not overdriven by large jumps of the required signal. It is important when using a fast control that interference pulses are blanked before reaching the filter module. Otherwise, these pulses would control the amplifier and thus blank the required signal.

However, after the level of the required signal decreases, the gain and the absolute level should increase more or less slowly according to the modulation mode. The following values can be used as orientation values for large level variations, whereas the values should be ten times slower in the case of small level variations: In the case of CW, the gain rise rate should be approximately 5 dB/ms, whereas SSB-values from 1 dB/ms to 0.1 dB/ms are found suitable. In the case of short time constants, a dynamic compression of the lower frequencies of the modulation signal takes place. For this reason, the time constant using conjunction with AM should be long, since only fading effects must be controlled. In the FM-mode it is possible for the time constant to be short, since a large AM-suppression is exhibited. Unfortunately, a compromise must be made here since a fast control will also cause interference due to phase modulation in the IF-amplifier.

The fall and rise times are determined by different components, and it is possible for them to be set virtually independent of another.

Let us examine the components and the effects which determine the time behaviour. The minimum fall time of the gain is determined by the signal delay in the IF-amplifier and control voltage amplifier, as well as by the charge times of the capacitors at the rectifier, and the discharge times of the capacitors in the control voltage line.

This time is especially of interest when the module is to be used without filter module.

The signal delay amounts to approximately 0.2 $\mu$s and can be classed as the dead-time of the control circuit. The transcient time of the IF-amplifier to half the voltage value is 5 $\mu$s. The charge time of the rectifier capacitor together with the filter link previous to the base of T 11 is at least 0.3 $\mu$s, and is level-dependent due to the base current of transistor T 11. The discharge time of the capacitors in the control voltage line is mainly determined by the value of $C_T$ and by the discharge current through T 11. This current is directly dependent on the level at the base. For this reason, the discharge time is level-dependent, and is small for large level variations. Capacitor $C_T$ should not exceed 4.7 $\mu$F, otherwise the discharge current will be greater than the maximum permissible collector current of T 11. A current limiting could be achieved using a resistor in the collector line of T 11.

A further delay is caused by the coupling capacitors and filter capacitors in the PIN-diode attenuator, and the filter links at gate 2 of the FETs. The delay time in the attenuator is very much greater than the delay times at gate 2 of the FETs. These are very different and amount to approximately 1.5 $\mu$s for transistor T 6, and approx. 10 $\mu$s for T 7. This guarantees that T 6 is firstly controlled, and that T 7 is not over-driven. The times are so short that the maximum rise times for the signal are determined by the bandwidth of the crystal filter so that the amplifier can be controlled without limiting.

With the aid of the RC-filter in front of the base of transistor T 11, it is possible to increase the fall (decay) time as required. However, the control circuit will become unstable at higher values, and will lead to a strong overshoot in the control characteristic, which will also lead to a »ringing« of pulse-type signals.

The recovery time of the AGC-circuit is determined by the time constant of $R_T$ and $C_T$ together with the filter capacitors in the control voltage line. In the case of $R_T = 820$ k$\Omega$, the minimum control time will be approximately 10 ms without $C_T$, and the maximum time of approximately 3.5 s for large level variations will be obtained with a value of $C_T = 4.7$ $\mu$F.

The gain rise times are dependent on the absolute value due to the non-linear control characteristic (Fig. 14 and 15), since the gain varies by approximately 6.5 dB/V in the control voltage range from 5.6 V to 3.5 V, and by approximately 37.5 dB/V in the control voltage range from 3 V to 1.2 V. Since the increase of the control voltage is made according to an exponential function with the time constant dependent on $C_T$ and $R_T$, this non-linear behaviour will be increased still further. This results in a relatively fast rise time of the gain in conjunction with high absolute levels, and a relatively low one with low absolute levels.

This time behaviour of the control is found to be very pleasant by the author on the VHF and microwave bands. The stations are immediately audible at a pleasant volume level and will not pump the AF-amplifier with the first syllable. After the signal disappears, the noise level of the receiver will increase slowly. A different control characteristic may be advisable for operation on the shortwave bands; this can be obtained by varying the value of capacitor $C_T$.

### 3.3.4. S-Meter

It is only possible to display the whole dynamic range of the IF-amplifier linearly on a meter when special detectors having a corresponding dynamic range are used. An example of this is the successive-detection with a logarithmic indicator such as described by DL 8 ZX in (19). Such a detector is provided in the panoramic receiver as shown in Figure 12.

This allows an exact measurement of the absolute level.

The dynamic range of the described concept corresponds to S0 to S9 + 46 dB when using the most common definition of S9 = 50 μV at the input of the receiver as used in amateur technology. With 6 dB per S-level, this corresponds to 16.6 S-points. This means that the pointer width of common meters would virtually correspond to one S-level.

In the case of the circuit shown in **Figure 18**, the control voltage is used for indication. Due to the non-linear control characteristic and the control voltage threshold at 0.1 μV at the input of the input circuit DJ 7 VY 002 (Figure 1), the indication range from 0 to 50 % will only cover the first three stages from S 1 to S 4. This large spread of the lower indication range has the advantage that it is more easily possible to give the signal report in »dB over noise«, which is more advisable for VHF-communications. It also allows the antenna to be adjusted more easily when receiving weak signals.

If strong signals are to be compared, it is possible for an attenuator to be used in the signal path to bring the level down to the most favorable indication range.
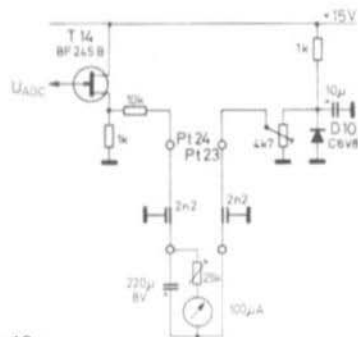


Fig. 18:
The S-meter reading is derived from the control voltage

The circuit given in Figure 18 does not possess any special features. The zero-point can be adjusted with the aid of the 4.7 kΩ resistor, and the 25 kΩ potentiometer is used to set the maximum value. Due to the good stability of the module, it is possible for the meter to be calibrated in μV. The disadvantage of the circuit is that signals below S 1 will not be indicated.

---

### 3.4. NOTCH FILTER

---

Amateur receivers are usually equipped with a Notch filter in the AF-amplifier for suppression of interfering carriers in the passband range. In the AF-range, such filters can be constructed with virtually ideal characteristics. The only disadvantage is that the interference carrier can control the IF-amplifier, and thus blank the required signal. It is therefore advisable for the suppression to be made in the IF-range between crystal filter and IF-amplifier.

In order to achieve a narrow-band suppression, it is necessary to use a filter having a high Q. This can only be achieved at IF-level when using a filter crystal. Crystals having a Q of 135 000 to 150 000, were used for the measurements.

Suitable circuits were given in (20) and (21). For comparison, experiments were made using a bridge filter and a T-filter with coupled inductances.
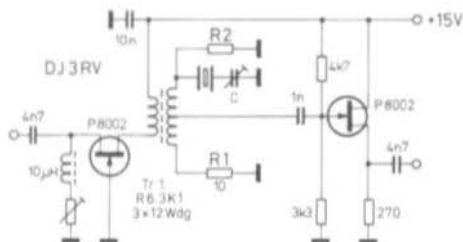
Fig. 19:
A Notch-filter at IF-level using a bridge
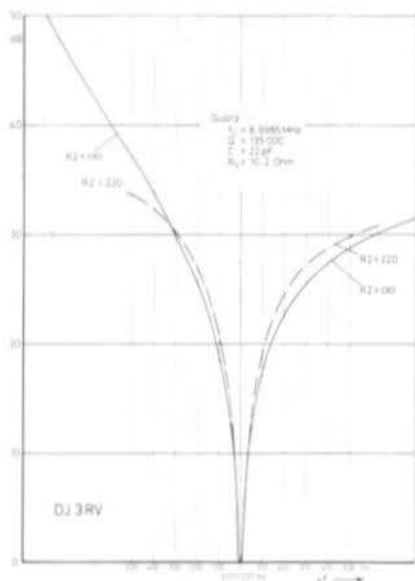circuit to obtain a large Notch-depth



Fig. 20:
The frequency response of the Notch-bridge
filter for various values of R 2 when select-
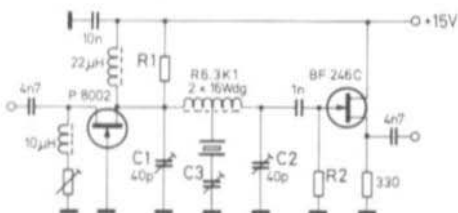ing a Notch-depth of 35 dB



Fig. 21:
A Notch-filter at IF-level as T-filter having
a wide variation range of the Notch-frequency

### 3.4.1. Bridge Filter

The circuit of the bridge filter is shown in
**Figure 19**, and the measured results in **Fig. 20**.

The secondary winding of Tr 1 forms a bridge
circuit together with R 1 and the equivalent re-
sistance $R_s$ of the crystal at series resonance,
which can be aligned with R 1 = $R_s$. The volt-
age at the center tap is then theoretically zero.

When using this circuit, a suppression of >
70 dB can be achieved, however, the filter is
then extremely narrow-band and the adjust-
ment will not be stable enough due to the tem-
perature behaviour of the components The
equivalent resistance $R_s$ of the circuit will also
change when the crystal is pulled with the ca-
pacitance C. This means that a large notch
depth is only possible within a low pulling
range of the crystal.

In the experimental circuit, the notch depth
was selected to be 35 dB with the aid of R 1. As
can be seen in the measured curve, a parallel
resonance of the crystal and Tr 1 will appear
without R 2, which will cause a great gain in-
crease of the circuit. This resonance is sup-
pressed with the aid of R 2 = 220 Ω since the
series circuit of R 1 and R 2 represents the
transformed load impedance for the first tran-
sistor. This has a gain of 1. With the series re-
sonance of the crystal, the load impedance is
mainly formed by the series circuit of $R_s$ and
R 1. The gain is thus reduced by 10 dB to 0.1.
This effect results in the improved slope steep-
ness of the filter curve when using the same
crystal.

### 3.4.2. T-Filter

The T-filter shown in **Figure 21** represents a
two-stage bandpass filter which is coupled via
the crystal impedance. Capacitors C 1 and C 2
determine the passband characteristics of the
filter outside of the series resonance of the cry-
stal. The notch frequency of the filter can be
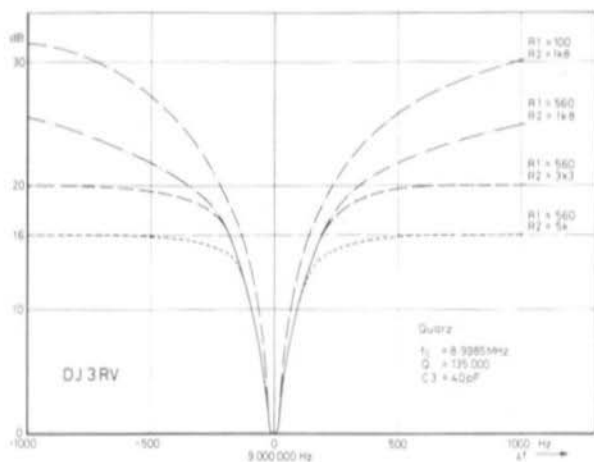varied with the aid of C 3 by pulling the crystal.

179

Fig. 22:
The frequency response
of the Notch-filter for
various source and load
resistances

The depth of the notch is dependent on the Q of the equivalent circuits and the crystal itself. Since the Q of the crystal is fixed, the overall Q can be varied with the aid of R 1 and R 2. **Figure 22** shows the measured curves for the various resistance values. The filter curves are relatively wideband, and for this reason it is advisable for two identical filters to be connected one behind the other. Since the notch depth does not vary as much as when using the bridge circuit, it is possible for the notch filter to be varied over the SSB bandwidth range.

## 3.5.
## LIMITING AMPLIFIER

Frequency modulated signals should be limit-

ed in order to improve the signal-to-noise ratio. This can be achieved by limiting with diodes, or directly using the base-emitter diode of the amplifier transistor. It is also possible to operate the transistor with a lower collector-emitter voltage which will also lead to limiting, since the transistor will then be driven into saturation.

Push-pull circuits such as differential amplifiers are used for balanced limiting. Limiter circuits made up from a chain of 6 to 8 differential amplifiers as used in FM broadcast receivers are not suitable for this concept. The available gain of these circuits is too high so that the noise signal would already be limited at the output of the controlled IF-amplifier. A single-stage differential amplifier is sufficient for this application. A differential amplifier requires a voltage of approximately 60 mV$_{p-p}$ at the differential input to obtain the limiting threshold. Since the output signal of the IF-amplifier is set
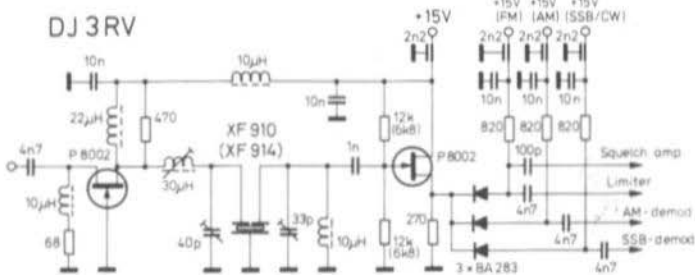


Fig. 23:
The selective buffer
amplifier with change-
over switching for the
various demodulators

to 10 mV, an additional amplifier will be required.

When using the buffer amplifier shown in **Figure 23**, a gain of approximately 15 dB is obtained at the same time as providing a further selectivity using an additional two-pole crystal filter. A filter XF 910 with $\pm$ 7.5 kHz bandwidth as already used in the receiver is suitable for this application. If the demodulator module is only to be used for narrow-band modulation modes, it is possible for filter XF 914 with $\pm$ 1.75 kHz bandwidth to be used here. At the output of the buffer, the required signal is switched to the associated demodulator with the aid of switching diodes.

A mixer circuit SO 42 P connected as differential amplifier is used as limiter, as shown in **Figure 24**. Any other differential amplifier having a wide bandwidth can be used in this circuit, however, the SO 42 P is also used here to keep the number of different components at a minimum. The limiter characteristic is shown in **Figure 25**.

## 3.6.
## FM DEMODULATOR

Since various frequency deviations are used for amateur communications, various circuits with differing discriminator characteristics were examined. The bandwidth requirement of the frequency modulated signal is given by the following rule of thumb:

$$B = 2 f_{Mod} + 2 \Delta f_T$$

where $f_{Mod}$ is the maximum modulation frequency, and $\Delta f_T$ is the frequency deviation.

Since the signal should have the lowest possible distortion, the bandwidth of the filter and the linear part of the discriminator characteristic should correspond to the signal bandwidth.

### 3.6.1.  PLL-Demodulator

When compared with other types of demodulators, PLL-demodulators should provide a
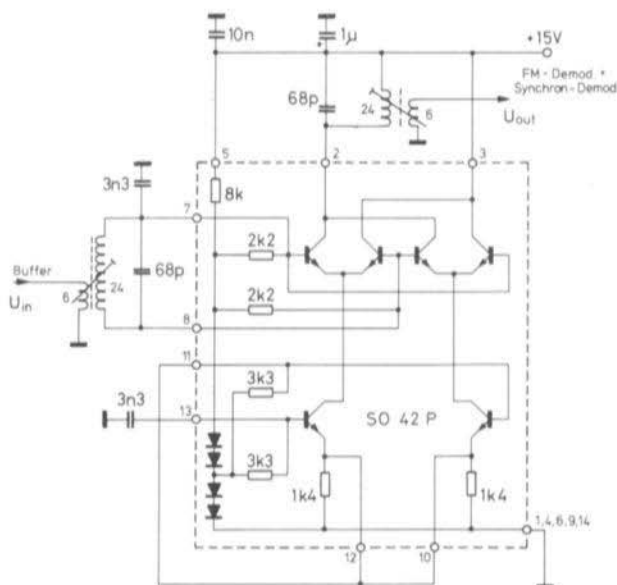


Fig. 24:
A limiter using a mixer
circuit SO 42 P switched
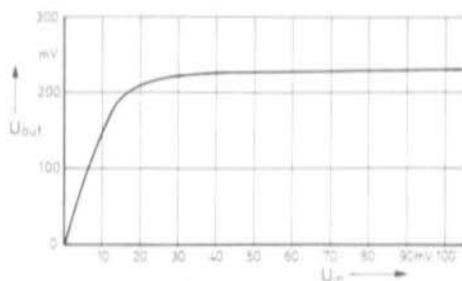as differential amplifier

Fig. 25:
The limiter function of the circuit
shown in Fig. 24

better AF signal-to-noise ratio at lower RF si-
gnal-to-noise ratios. This is valid for lower in-
termediate frequencies, however, the author
could not measure any advantages when
using the PLL-circuit XR 215 (Exar) for an IF of
9 MHz. The intrinsic noise of the VCO in the cir-
cuit is too great. This can be improved by using
a crystal as frequency-dependent component.
The discriminator curve will, however, only
have a hump spacing of ± 170 Hz when using
a crystal type XF 900. The values of ± 1 kHz
given by the manufacturer in (22) cannot be
achieved.

### 3.6.2. Phase Detector

A number of circuits have been described in
this magazine e.g. (23), using phase detectors
and crystal filter as phase shifter for FM demo-
dulation, which means that the following can
be limited to experiments on circuits having a
lower hump spacing. The SO 42 P is to be
used as quadrature demodulator using one
dual as phase shifter. The circuit is given in
Figure 26.

The emitter follower connected between
phase shifter and SO 42 P is only used as im-
pedance converter since the input of the de-
modulator module at point 8 has too low an im-
pedance.

The signal is taken from the limiter at low impe-
dance and is fed as switching signal to pin 11.
The drive of the phase-shift filter is made at
high impedance using an LC-transformation.
The center frequency is adjusted with the aid
of the capacitor, whereas the output LC-circuit
determines the linearity of the discriminator
characteristic, together with the real load pro-
vided by the base voltage divider and the input
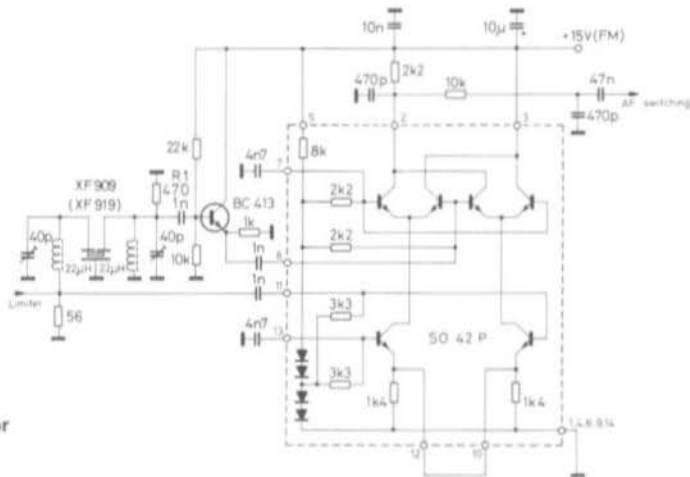impedance of the transistor (as well as possi-
bly R 1).



Fig. 26:
The SO 42 P is connected
as coincidence demodulator
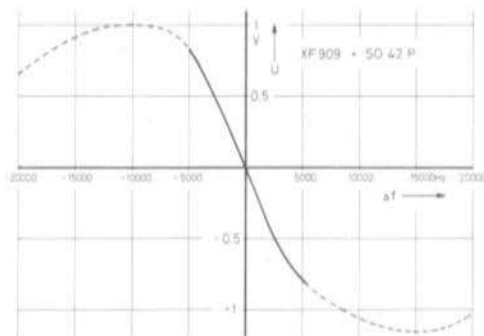and uses a crystal filter
for phase shift

**Fig. 27:**
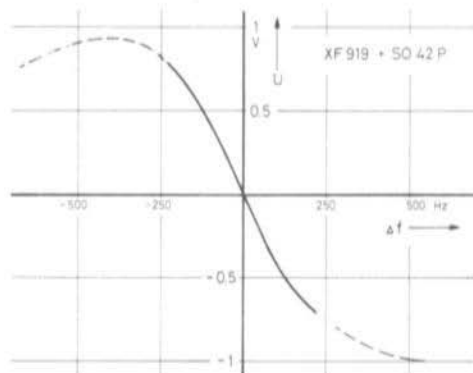**The discriminator characteristic for**
**5 kHz deviation**



**Fig. 28:**
**The discriminator circuit equipped with XF 919**
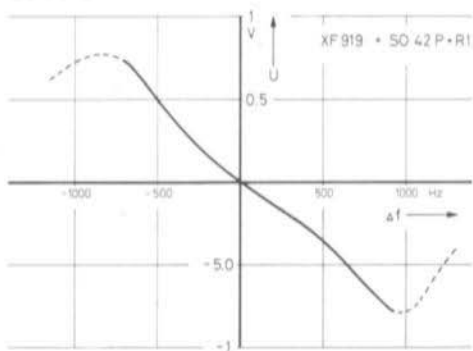**allows a deviation of 250 Hz and is thus suitable**
**for RTTY**



**Fig. 29:**
**The discriminator characteristic can be increased**
**to 800 Hz by adding the load resistor R 1**

The dual crystal filter XF 909 will result in the discriminator characteristic shown in **Fig. 27** if R 1 is not connected. Up to a bandwidth of 10 kHz, the distortion factor is less than 3 %. Such values can be achieved down to a bandwidth of 500 Hz without R 1, and for a bandwidth of 1.6 kHz with R 1 = 470 $\Omega$ when using a dual filter XF 919. The measured values are shown in **Figures 28 and 29**.

### 3.6.3. Squelch Circuit

The squelch circuit is to block the AF-channel until a signal of sufficient field strength is present to ensure that a noise-free signal can be received. There are various methods of generating the control signal. The noise at the demodulator can be coupled out via a filter, amplified and rectified as was described in (24). If a signal is received, the noise level will decrease and the AF-amplifier is opened.

Another method is to obtain a control signal from the IF-voltage which can be tapped off before the limiter. This could be achieved using the circuit given in **Figure 30**.

The IF-signal is amplified in the transistor stage and rectified in a voltage-doubler circuit. The differential amplifier operates as a comparator that compares the rectified signal to a voltage set with the aid of the 10 k$\Omega$ potentiometer. As long as the voltage adjusted at the potentiometer is greater than the rectified signal voltage, the right-hand transistor conducts and the voltage drop across the collector resistor will block the AF-amplifier. However, this squelch circuit will only operate with input signals up to the control voltage threshold, since in excess of this the IF-voltage is maintained at a constant level.

Furthermore, the control voltage can be used as control signal. In this case, it is advisable that the control commences at the noise threshold. This is not possible in the described concept where low-noise input stages are used. The squelch can therefore only be opened by signals which are able to actuate the control circuit.
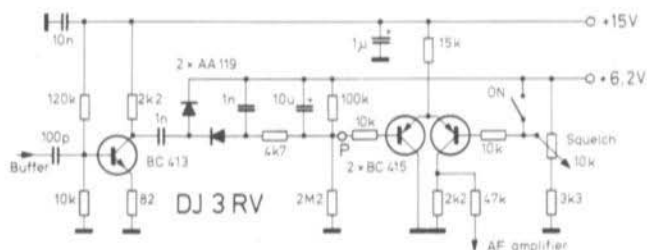
Fig. 30:
The control voltage
generator for the
squelch

Technically speaking, this can be achieved easily if the circuit given in Figure 30 is disconnected at point P and connected to the source of the control transistor of the S-meter circuit (Figure 18).

## 3.7. AM-DEMODULATION

Mainly two principles are used for AM-demodulation. The first is the envelope demodulation using a rectifier circuit, and the second is the reconversion of the AM-signal using the carrier (synchronous demodulation). Both types of demodulator were tested and are to be described individually.

### 3.7.1. Push-Pull Demodulator

The most simple form of AM-demodulation is an envelope demodulator using diodes such as used in the control voltage rectifiers shown in Figure 17. Due to the relatively high threshold voltage of the diodes, low RF-voltages can only be demodulated with a high degree of distortion.
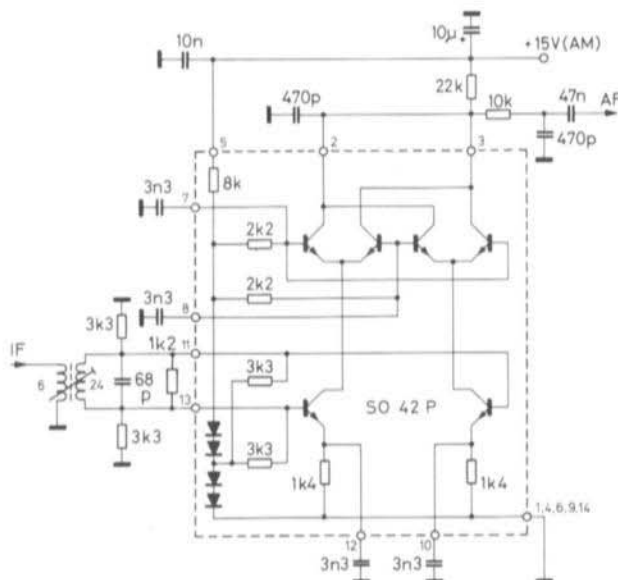


Fig. 31:
The AM-envelope demodulator
using a push-pull circuit

It is possible using a bias current for the diodes to be operated in class B so that low RF-voltages can also be demodulated at low distortion. However, the operating point is then very temperature-dependent. DJ 4 BG showed in (25) that it is possible to carry out a temperature-compensated rectification using the base-emitter diodes of transistors. This type of circuit was built up in push-pull using a SO 42 P as shown in **Figure 31**. The input signal is balanced using the coupled resonant circuit. The transformation ratio has been selected so that the input impedance of the circuit is approximately 50 Ω. The base-emitter diodes between pins 13 and 12, as well as 11 and 10 are connected as push-pull rectifiers. The base bias voltage is derived from two series-connected diodes, and is halved using the internal and external 3.3 kΩ resistance so that the rectifier operates in class B. The internal 1.4 kΩ resistors ensure a good balance. A very good temperature compensation is achieved using these measures. The author did not experiment to find out whether an improvement could be achieved by reducing the current flowing through the bias diodes.

The rectified signal is taken via the collectors and the transistors connected as adding stage from points 2 and 3. The circuit operates at a low distortion factor for input signals from 3 mV to 100 mV. For signals in excess of 100 mV, an overdrive condition will exist for the transistors in the adding stage. This can be checked to see whether any voltage breakdown can be seen with an oscilloscope connected to points 7 and 8.

## 3.7.2. Synchronous Demodulator

The synchronous demodulator is a mixer circuit in which the AM-signal is mixed with a signal that is synchronous to the carrier frequency. A synchronous signal can be achieved with the aid of a PLL-circuit or simply with the aid of a limiter. All circuits that are used for converting SSB signals are suitable as mixer circuit if the synchronous signal is injected instead of the BFO-signal, as is shown in the circuit diagram of the SSB demodulator.

Synchronous demodulators have a greater dynamic range and less distortion than envelope

Fig. 32:
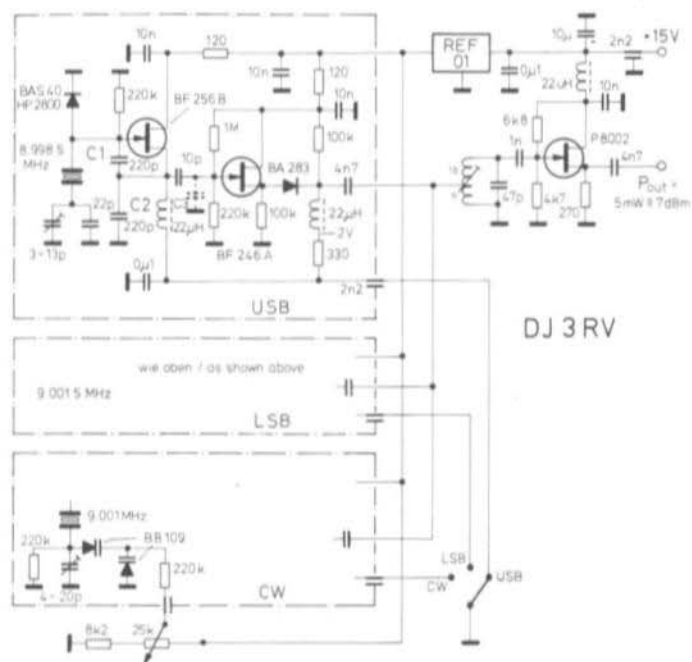The mixer circuit for demodulation of AM, SSB and CW signals



185
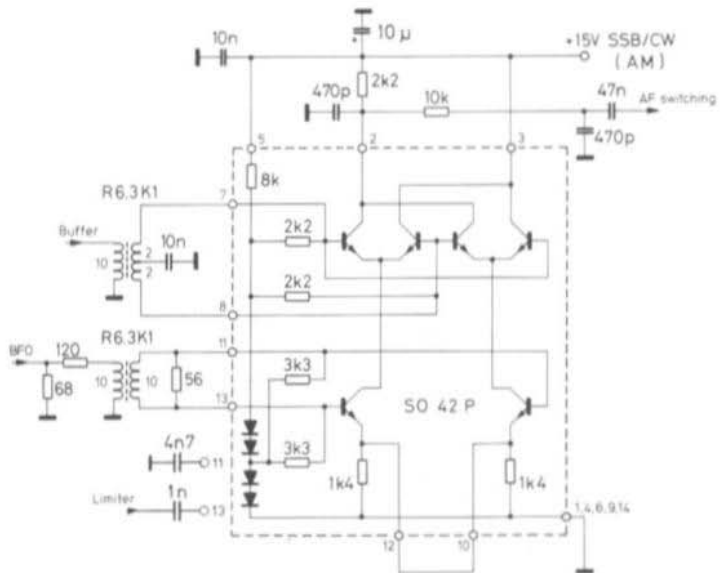
Fig. 33:
A low-noise BFO
for three switch-
able frequencies
and a maximum
output power
of 5 mW

DJ 3 RV

demodulators. For this reason, such a demo-
dulator was planned as demodulator in the ori-
ginal concept. However, it was found that the
generation of a synchronous carrier signal with
a limiter provided too great a degree of ampli-
tude and phase interference at low input levels
due to the interfering pulses. The envelope de-
modulator as shown in Figure 31 provides a si-
gnal with less interference.

## 3.8.
## SSB/CW DEMODULATOR

The demodulation of an SSB-signal is made
by converting it with a signal having the same
frequency as the original carrier signal. Since a
high carrier suppression is used in amateur
SSB-communications, it is not possible to re-
cover the carrier from the input signal, and this
means that an auxiliary (BFO) signal must be
generated. This BFO-signal is mixed to the in-
put signal in a mixer circuit and the AF-signal is

coupled out via a low-pass filter. All conventio-
nal circuits can be used as mixer, and a
double-balanced diode mixer such as the
IE 500 requires the lowest external circuitry.
However, it requires a relatively high BFO-le-
vel of at least 5 mW.

The circuit given in **Figure 32** shows a mixer
equipped with a SO 42 P in a standard circuit.
The received signal from the buffer amplifier is
balanced in a toroid core transformer and fed
to pins 7 and 8; the BFO-signal is fed via an at-
tenuator in a balanced manner to pins 11 and
12. The attenuator is provided as a precautio-
nary measure for levels greater than 1 mW,
since the data sheet does not give any details
regarding the maximum permissible input po-
wer at pins 11 and 13. Measurements showed
that the conversion gain did not increase con-
siderably for BFO-levels in excess of − 6 dBm.
At greater levels, the suppression of the BFO
signal at the signal input and AF-output were
considerably less. The AF-signal is coupled
out from pin 2 via a low-pass filter comprising a
10 kΩ resistor and 470 pF capacitor.

The mixer circuit is very sensitive and can be driven with considerably lower levels of the input and BFO signals if tapped resonant circuits are used instead of the toroid core transformers. Since the higher level was available in the overall concept, toroid core transformers were used on the PC-board also for compactness.

## 3.9.
## B F O

Since the BFO was also used as signal source for the intermodulation measurements on the crystal filter, a very low-noise circuit was developed having a low harmonic content. As can be seen in **Figure 33**, separate oscillators are provided for the various BFO-frequencies that can be switched in as required.

A Colpitts-circuit equipped with a junction FET

is used as oscillator. The crystal oscillates in parallel resonance and is coupled to the FET with the aid of C 1 and C 2. In the case of crystals having a lower Q, the coupling can be increased by increasing the value of C 1, or decreasing the value of C 2. The Schottky diode connected from gate to ground is used for amplitude limiting by negatively charging capacitor C 1 at the gate on increasing amplitude, which in turn drives the operating point of the FET into a range of lower slope.

The exact frequency adjustment is made using a pulling capacitance in series with the crystal. The CW-crystal frequency can be adjusted to cover the CW-filter bandwidth with the aid of a varactor diode and a 5.6 pF coupling capacitor. If a larger frequency range is required, it is necessary to use two diodes since although the variation range of the individual diode is increased on increasing the coupling capacitance, the diode will be driven into the forward direction by the RF-amplitude.
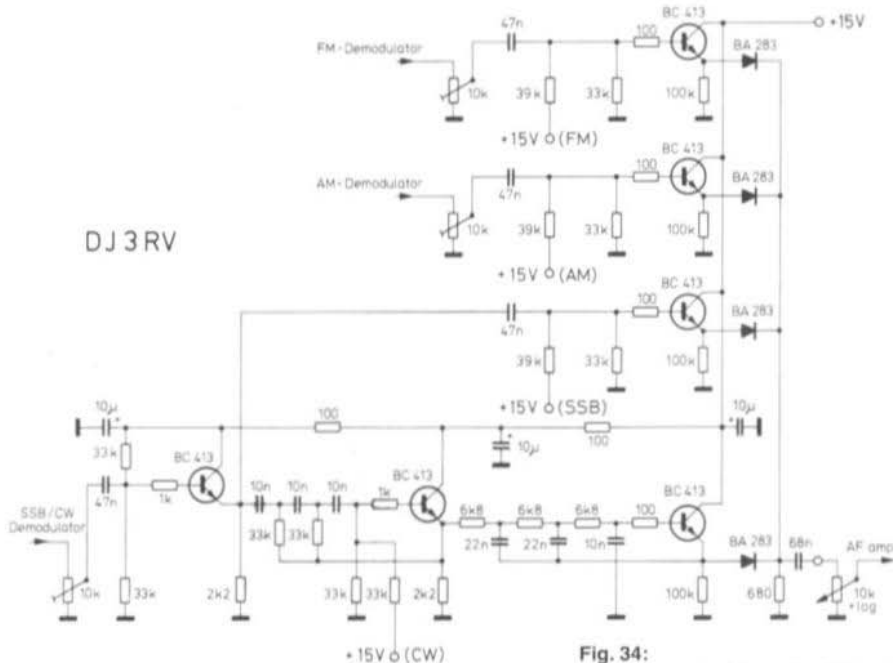


DJ 3 RV

Fig. 34:
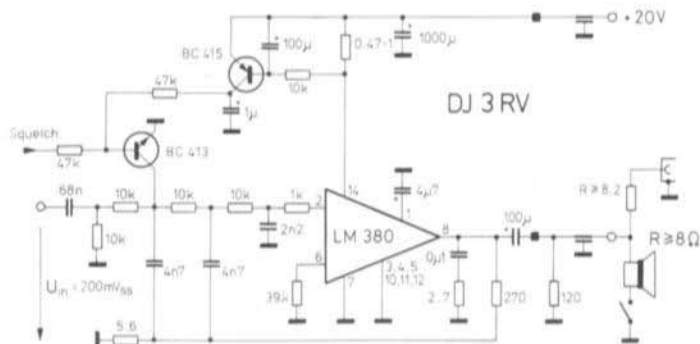The audio switching with CW-audio filter

Fig. 35:
The AF-amplifier with
short-circuit protection
and squelch switch

The signal is coupled out via a 10 pF capacitor at the source follower. Since the oscillator amplitude is dependent on the large spread of the slope of the first FET, an amplitude alignment can be carried out with the aid of C 3 which is used as capacitive voltage divider, in order to ensure that all three oscillators provide the same amplitude at the output.

Only one of the oscillators may be switched on at one time. The two other oscillators are blocked with the aid of switching diodes type BA 283.

The tapped resonant circuit improves the harmonic suppression, which means a maximum of 5 mW having a harmonic rejection of $>$ 45 dB can be coupled out after the source follower.

## 3.10.
## AF-AMPLIFIER

As can be seen in **Figure 34**, the demodulated AF-signals are switched to the AF-amplifier shown in **Figure 35** with the aid of emitter followers and switching diodes. Active filters as described by DJ 4 BG (26) are used as AF-filters.

The AF-amplifier does not possess any special features. Since the integrated circuit does not have any internal current limiting as protection against overdrive and short-circuit at the output, it is possible to use a current limiting to the squelch switching transistor equipped with a BC 415. This will not be required if it is not possible to short-circuit the output.

The squelch circuit is obtained by short-circuiting with the aid of the BC 413. When using a LM 380 as AF-amplifier, the transistor can be connected to pin 1 in the same manner as described by DC 3 NT in (27).

## 3.11.
## IF OUTPUT COUPLING

High demands are placed on an IF-output. Not only must this output be insensitive to any mismatch, even short or open circuit, but also have a low reaction. Any external signals, such as the oscillator of an external mixer, may not be injected into the circuit. The circuit shown in **Figure 36** satisfies these demands. The output coupling of the IF-signal is made from the collector of the first amplifier of the control-voltage circuit. The signal is then passed through a filter and a low reactive cascade of two FETs.
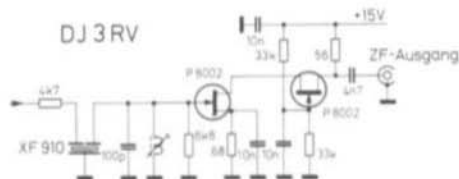
DJ 3 RV

Fig. 36:
A low-reactive IF-coupling

The input of the filter is matched with resistors. The output matching is realized with a 6.8 kΩ resistor, and the reactive components are compensated for by the LC-circuit.

When using a drain resistor of 56 Ω, the cascade stage will exhibit a gain of approximately 1, which means that the IF-signal will be 25 mV with the IF-amplifier controlled.

The low reaction is achieved due to the low-sensitivity to mismatch of the cascade circuit and due to the voltage division of the matching resistor at the input of the filter and collector resistor in the control voltage amplifier.

The isolation amounts to approximately 60 dB in the passband range of the filter and increases to 90 dB in the stopband range.

## REFERENCES to part 3

(16)  J. Schürmann, DJ 1 SK:
      Modern FETs for HF
      cq-DL 1973, edition 11, pages 418-422

(17)  J. Schürmann, DJ 1 SK:
      Die PIN-Diode und ihre Anwendung
      Funktechnische Arbeitsblätter Re 91
      Funkschau 1973, edition 1, pages 37-40

(18)  J. Schürmann, DJ 1 SK:
      Der BF 910 als rauscharmer großsignal-
      fester Dual Gate MOS-FET mit hoher
      Steilheit für Verstärker und Mischan-
      wendungen bis 500 MHz
      Applikationsbericht 51 in
      Applikationsbuch Volume 3 (UHF/VHF)
      Texas Instruments Deutschland GmbH,
      Freising 1978

(19)  E. Berberich, DL 8 ZX
      A Spectrum Analyzer for Amateur
      Applications
      VHF COMMUNICATIONS 9,
      edition 2/1977, pages 109-120

(20)  AEG-Telefunken:  Nullstellenfilter
      Telefunken-Laborbuch Vol.6 (1980),
      pages 124-133

(21)  H. Matthes:
      Crystal band-stop filters with improved
      spurious resonance behaviour
      Int.J.of Circuit Theory and Applications,
      Volume 4, pages 25-42 (1976)

(22)  EXAR:  Phase-locked loop data book
      Sunnyvale (1980)

(23)  J. Kestler, DK 1 OF:
      A FM Transceiver for the 2 m Band
      Part 1: The Receiver
      VHF COMMUNICATIONS 11,
      Edition 1/1979, pages 44-53

(24)  G. Rühr, OH 2 KT:
      A Miniature Receiver for the 2 m Band
      VHF COMMUNICATIONS 7,
      Edition 4/1975, pages 239-243

(25)  D. E. Schmitzer, DJ 4 BG:
      AM-Demodulators using Silicon Semi-
      conductors
      VHF COMMUNICATIONS 3,
      Edition 3/1971, pages 190-193

(26)  D. E. Schmitzer, DJ 4 BG:
      Active Audio Filters
      VHF COMMUNICATIONS 1,
      Edition 4/1969, pages 218-235

(27)  R. Tellert, DC 3 NT:
      A System for Reception and Display of
      METEOSAT Images  —  Part 2
      VHF COMMUNICATIONS 11,
      Edition 4/1979, pages 194-202

# An Amateur-Television Transmitter for Home Construction
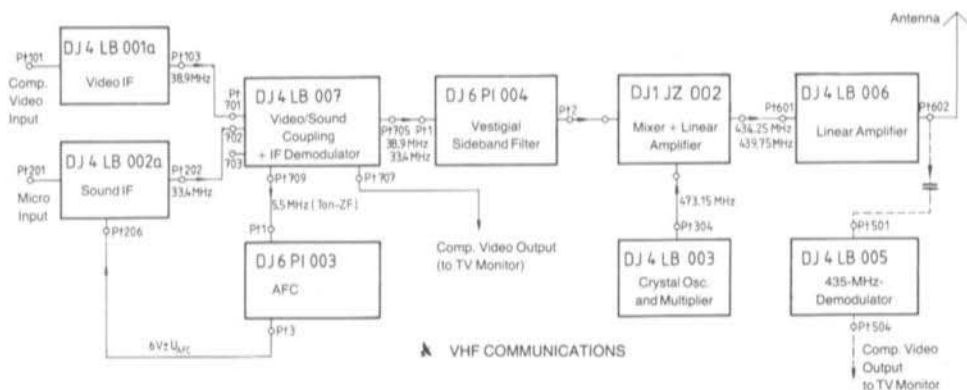


A television transmitter built from modules described in VHF COMMUNICATIONS is shown in the above **block diagram**. Each function is realised on an individual PC-board. Each PC-board is built into its own tinned-metal box, which leads to a very clean operation without unwanted stray coupling and without problems caused by radiation. Each module may be aligned and tested on its own. All this encourages the home constructor since it makes it easy to understand the different functions, and it finally leads to a high-value ATV transmitter to which all possible video sources (black/white or color) may be connected.

For an amplification of the transmit power, a variety of linear amplifiers for the 70 cm band may be used (not FM »linears« !), whereby care should be taken to adjust the drive so that the output power does not exceed half the PEP value of the SSB mode.

The ATV modules listed have been published by three authors. The descriptions are detailed and will enable successful duplication. They are to be found in the following **editions of VHF COM-MUNICATIONS:**

| | | | |
|---|---|---|---|
| VHF COMMUNICATIONS | 1/1973 | VHF COMMUNICATIONS | 4/1977 |
| VHF COMMUNICATIONS | 2/1973 | VHF COMMUNICATIONS | 3/1981 |
| VHF COMMUNICATIONS | 2/1976 | **This set of 6 editions is available** | |
| VHF COMMUNICATIONS | 1/1977 | **at DM 24.—** | |

**Individual kits:**

| | | | | | | |
|---|---|---|---|---|---|---|
| DJ 4 LB 001a | kit, complete | DM 98.— | DJ 6 PI 004 | ready-to-operate | DM | 115.— |
| DJ 4 LB 002a | kit, complete | DM 99.— | DJ 4 LB 003 | kit, complete | DM | 92.— |
| DJ 4 LB 007 | kit, complete | DM 90.— | DJ 1 JZ 002 | kit, complete | DM | 131.50 |
| DJ 6 PI 003 | kit, complete | DM 50.— | | | | |

**Set of complete kits for the 70 cm ATV transmitter (without power amplifier)**
comprising DJ 4 LB 001a, DJ 4 LB 002a, DJ 4 LB 007, DJ 6 PI 003,
DJ 6 PI 004, DJ 4 LB 003, DJ 1 JZ 002                                    **DM 695.—**

# VHF
# *communications*

offers ...

## A System for Reception and Display of Weather-Satellite Images using a digital scan converter/storage module with 256 lines, 256 pixels and 64 grey levels

As a modern replacement for the DC 3 NT video processor, VHF COMMUNICA-TIONS is now able to offer a digital scan converter with the above mentioned features. The 2400 Hz subcarrier is fed from the VHF receiver (DC 3 NT 003/004), processed and stored in the scan converter, and the CCIR video output can be displayed on any suitable monitor. The scan converter itself consists of two PC-board modules and will be published in the next two editions. We can, however already offer these modules in advance since they will be available from January 1983.

All these modules are available as kits, ready-to-operate aligned modules, or as complete equipment in cabinets.
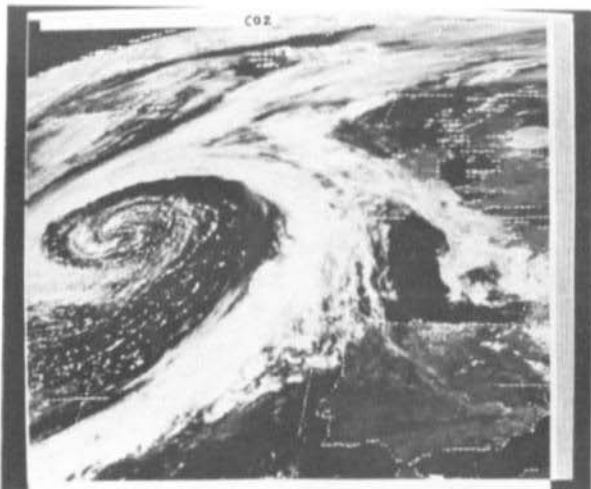
## A) A complete system as kits

| Part in the system | Described in Edition | Kit designation | Art.Nr. | Kit DM | Total DM |
|---|---|---|---|---|---|
| 1. **Parabolic antenna**, 1,1m diam., 12 segm. to be screwed or riveted together | 3/1979 | **Parabolic antenna kit** | 0098 | 180.00 | |
| | | **Riveting machine + rivets** | 005 D | 93.00 | |
| | | **1.7 GHz Cavity radiator kit** | 0091 | 90.00 | |
| | | | | Total: | 363.00 |
| 2. **Low-noise amplifier for 1.7 GHz** (Originally described for use at 2.4 GHz, this unit is tuned to 1.7 GHz) | 1/1980 | **DJ6PI010** | 6565 | 225.00 | 225.00 |
| 3. **METEOSAT Converter**, consisting of two modules — Output first IF = 137.5 MHz) | 4/1981 | **DJ1JZ 003** | 6705 | 189.00 | |
| | 1/1982 | **DJ1JZ 004** | 6714 | 185.00 | |
| | | | | | 360.00 |
| 4. **VHF Receiver**, frequency range: 136-138 MHz, Output: 2400 Hz sub-carrier | 4/1979 | **DC3NT 003** | 6141 | 225.00 | |
| | 1/1980 | **DC3NT 004** | 6145 | 80.00 | |
| | | | | | 305.00 |
| * 5. **Digital scan converter** (256 x 256 x 6 Bit) | 4/1982 | **YU3UMV 001** | | total | 675.00 |
| | 1/1983 | **YU3UMV 002** | | | |

## B) A complete system as aligned ready-to-operate PCB-modules

| | | | |
|---|---|---|---|
| **Cavity radiator** for above parabolic antenna | | 0092 | 150.00 |
| **VHF receiver** for 136-138 MHz, DC3NT 003 | | 6731 | 395.00 |
| **Oscillator for VHF receiver**, DC3NT 004 | | 6732 | 168.00 |
| * **Digital scan converter** (256 x 256 x 6 Bit) | | total | 1150.00 |

## C) A complete system, ready-to-operate in cabinets

| | | |
|---|---|---|
| **Parabolic antenna**, 12 segments, riveting machine and rivets, and cavity radiator (ready-to-operate) | | 423.00 |
| **METEOSAT converter** with GaAs-FET preamplifier and mixer, 2 channels, in casing | 3026 | 645.00 |
| **Antenna** for orbiting satellites, DJØBQ-137 | | 198.00 |
| Power combiner for above, AT-137 | | 98.00 |
| * **6-channel VHF receiver** in cabinet, programmed for: 137,130 / 137,300 / 137,400 / 137,500 / 137,620 / 137,850 MHz | | 1298.00 |
| * **Digital scan converter**, 256 x 256 x 6 Bit, with control electronic, in cabinet | | 1980.00 |
| **Video monitor**, black/white, with 31 cm C.R.T. | | 550.00 |

\* From January 1983

# *Space and Astronomical Slides*

## Informative and Impressive

VHF COMMUNICATIONS now offers sets of phantastic slides made during the Gemini, Apollo, Mariner, and Voyager missions, as well as slides from leading observatories. These are standard size 5 cm x 5 cm slides which are framed and annotated.

Prices plus DM 3.00 for post and packing.

### Sets of 5 NASA-slides DM 8.50 per set

| | |
|---|---|
| Set 8103 | Apollo 11: Earth and Moon |
| Set 8104 | Apollo 11: Man of the Moon |
| Set 8105 | Apollo 9 and 10: Moon Rehearsal |
| Set 8106 | From California to Cap Canaveral |
| Set 8107 | Apollo 12: Moon Revisited |
| Set 8108 | Gemini Earth Views |
| Set 8109 | Apollo 15: Roving Hadley Rille |
| Set 8110 | Apollo 16: Into the Highlands |
| Set 8111 | Apollo 17: Last voyage to the moon |
| Set 8112 | Apollo 17: Last Moon Walks |
| Set 8113 | Mariner 10: Mercury and Venus |
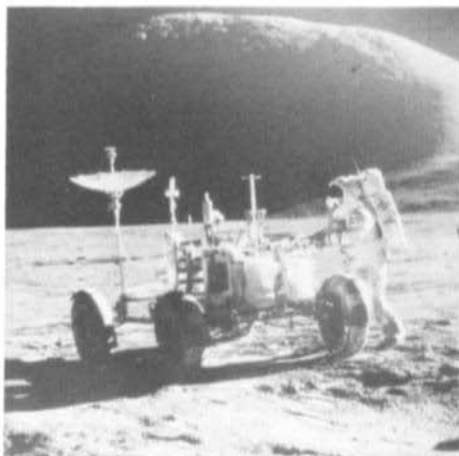
### Set 8147 »Jupiter encountered« 20 slides of VOYAGER 1 & 2 DM 35.00

1. Jupiter and 3 satellites 2. The giant planet 3. Jupiter, Io and Europa 4. The Red spot 5. The Red spot in detail 6. The swirling clouds 7. Io and a white oval 8. The neighbourhood of the Red spot 9. The rings of Jupiter 10. The Gallilean satellites 11. Amalthea 12. Callisto 13. Impact feature on Callisto 14. Eruption on Io 15. Io full disc 16. Europa close-up 17. Europa distant view 18. Ganymede close-up 19. A distant Ganymede 20. The Iovian system

### Set 8100 »Saturn encountered«, 20 VOYAGER-1 slides DM 35.00

1. Saturn and 6 of its moons 2. Saturn from 11 mio miles 3. Saturn from 8 mio miles 4. Saturn from 1 mio miles 5. Saturn and rings from 900.000 miles 6. Saturn´s Red spot 7. Cloud belts in detail 8. Dions against Saturn 9. Dione close-up 10. Rhea 11. Craters of Rhea 12. Titan 13. Titan's polar hood 14. Huge crater on Mimas 15. Other side of Mimas 16. Approaching the rings 17. Under the rings 18. Below the rings 19. »Braided« F ring 20. Iapetus

### Set 8148 »VOYAGER 2 at Saturn«, 20 VOYAGER-2 slides DM 35.00

1. VOYAGER 2 approaches 2. Clouds & rings 3. Storms & satellites 4. Cyclones, spots & jet streams 5. Convective regions 6. Atmospheric disturbance 7. Rings & shadows 8. The »C« ring 9. Ring details 10. The »A« ring 11. Looking back on Saturn 12. Titan – night side 13. Titan – atmospheric bands 14. The »F« ring 15. Hyperion close-up 16. Iapetus revealed 17. Enceladus explored 18. The Tethys canyon 19. The »F« ring structure 20. Within the Enke division

### Set 8101 »From Here to the Galaxies«, 20 astronomical slides DM 35.00

1. Moon – eastern limb 2. Moon – NE limb 3. Comet IKEYA SEKI 4. Trapezium 5. »Sunflower« planetary nebula in Aquarius 6. Nebula in Cassiopeia 7. North America nebula 8. Sagittarius star cloud 9. Spiral galaxy in Triangulum 10. Sp. gal. in Canes venatici 11. Sp. gal. in Coma Berenices 12. Sp. gal. in Leo 13. Edge-on sp. gal. in Virgo 14. Sp. gal. in Canes Venatici 15. Sp. gal. in Camelopardalis 16. Sp. gal. in Lynx 17. Sp. gal. in Pegasus 18. U.S. Naval Observatory Flagstaff, Ar. 19. 6-inch transit telescope 20. 61-inch reflector

### Set 8102 »The Solar System«, 20 NASA/JPL slides DM 35.00

1. Solar System 2. Formation of the Planets 3. The Sun 4. Mercury 5. Crescent Venus 6. Clouds of Venus 7. Earth 8. Full Moon 9. Mars 10. Mars: Olympus Mons 11. Mars: Grand Canyon 12. Mars: Sinuous Channel 13. Phobos 14. Jupiter with Moons 15. Jupiter Red Spot 16. Saturn 17. Saturn Rings 18. Uranus and Neptune 19. Pluto 20. Comet Ikeya-Seki.

### Set 8149 »The Sun in action«, 20 NASA/JPL slides DM 35.00

1. Sun in Hα light 2. Total Solar eclipse 3. Outer corona 4. Corona from SMM satellite 5. Corona close-up 6. Solar magnetogram 7. Active regions in X-radiation 8. X-ray corona 9. A coronal hole 10. Solar flare 11. Active Sun 12. Eruptive prominence 13. Gargantuan prominence 14. Eruptive prominence 15. Huge Solar explosion 16. Prominence in action 17. Sun in action 18. Magnetic field loops 19. Prominence close-up 20. Chromospheric spray

### Set 8144 »Space shuttle«, 12 first-flight slides DM 24.00

1. STS1 heads aloft 2. View from the tower 3. Tower clear 4. Launch profile 5. Payload bay open 6. STS control Houston 7. In orbit, earth seen through the windows 8. Bob Crippen in mid-deck 9. John Young 10. Approaching touchdown 11. After 54.5 hours in space Columbia returns to Earth. 12. Astronauts Crippen and Young emerge after the successful mission